Stony Brook University

The Role of Dynamic Muscle Contractions on Bone Loss and Muscle Atrophy in a Functional Disuse Mouse Model

A Thesis Presented

By

Adiba Mir Ali

To

The Graduate School

In Partial Fulfillment of the

Requirements

For the Degree of

Master of Science

In

Biomedical Engineering

Stony Brook University

December 2007

STONY BROOK UNIVERSITY

THE GRADUATE SCHOOL

Adiba Mir Ali

We, the thesis committee for the above candidate for the

Master of Science degree,

Hereby recommend acceptance of this thesis.

Yi-Xian Qin, Ph.D (Thesis Advisor)
Professor, Department of Biomedical Engineering

Stefan Judex, Ph.D
Associate Professor, Department of Biomedical Engineering

Brigitte Demes, Ph.D.
Professor, Department of Anatomical Sciences

This thesis is accepted by the Graduate School

Lawrence Martin
Dean of the Graduate School

ABSTRACT OF THE THESIS

The Role of Dynamic Muscle Contractions on Bone Loss and Muscle Atrophy in a Functionally Disuse Mouse Model

By

Adiba Mir Ali

Master of Science

In

Biomedical Engineering

Stony Brook University

2007

The highly dynamic musculoskeletal system is known to adapt to changes in its mechanical environment. These adaptations can include enhancement of the tissue's native function upon increased demand, or devastating consequences when exposed to the disuse environment. Thus, there is a need to investigate mechanical loading regimes that simultaneously prevent bone loss and muscle atrophy. Bone fluid flow has been shown to be induced during mechanical loading, and is believed to be a critical mediator of bone adaptation. It has been proposed that intramedullary pressure gradients and subsequently, bone fluid flow, can be regulated by skeletal muscle dynamics. The objective of this thesis was to investigate the role of dynamic muscle contractions as a preventive treatment for musculoskeletal disuse. The optimal loading parameters required for such a treatment are unclear; therefore, the two studies presented here examined the frequency specificity and the role of rest-insertions during muscle

stimulation. The effect of these parameters on bone morphological adaptation, mechanical strength, and muscle morphology was evaluated.

In the first study, a range of frequencies of muscle stimulation was tested at 1 Hz, 20 Hz, 30 Hz and 50 Hz. The strongest response in trabecular and cortical morphology were observed at 20 Hz and 50 Hz stimulations. Muscle stimulations demonstrated significant attenuation of trabecular bone volume fraction at 1 Hz (+34%, $p<0.05$), 20 Hz (+47%, $p<0.01$), 30 Hz (+27%, $p<0.05$), and 50 Hz (+48%, $p<0.01$). Cortical area also showed increasing trends upon muscle stimulation at 1 Hz (+6%, $p<0.05$), 20 Hz (+7%, $p<0.05$), 30 Hz (+8%, $p<0.05$), and 50 Hz (+10%, $p<0.01$). Significant differences between signal frequencies were observed in trabecular connectivity density (50 Hz > 30 Hz, $p<0.05$) and the structural model index (20 Hz > 30 Hz, $p<0.05$). Mechanical properties of the bone were enhanced when compared with hind limb suspension control, demonstrated by attenuation of tissue stiffness at 1 Hz (+6%), 20 Hz (+17%, $p<0.05$), 30 Hz (+15%), and 50 Hz (+13%) and maximal force at 1 Hz (+11%), 20 Hz (+23%), 30 Hz (+11%), and 50 Hz (+28%, $p<0.05$). Mechanical testing demonstrated strong attenuation within a similar range, as bone stiffness was enhanced at 20 Hz frequency, while maximal force experienced was greatest at 50 Hz. Muscle fiber CSA was attenuated upon muscle stimulations at 1 Hz (+13%), 20 Hz (+38%), 30 Hz (+45%, $p<0.05$), and 50 Hz (+31%), with significant changes only at 30 Hz. This study demonstrated that the high frequency range between 20 Hz to 50 Hz generated significant changes in muscle and bone.

The second study investigated the influence of a short, 5 minute recovery period inserted between two 5 minute stimulation bouts, during a 20 Hz frequency signal. Trabecular bone volume fraction showed slightly stronger responses with the continuous

signal (+47%, $p<0.01$; +35%), while cortical area showed stronger responses with the rest-inserted signal (+7%, $p<0.05$; +10%, $p<0.01$). Mechanical strength assessment suggests that rest-insertions do have stronger potential to attenuate disuse consequences. Maximal force was significantly enhanced with rest-insertions (+42%, $p<0.01$). Muscle cross sectional area results also showed strong attenuation (+44%, $p<0.05$) with rest-insertions. Overall, these results suggest that the musculoskeletal response to skeletal muscle dynamics do vary with loading frequency and recovery periods, and thus, may potentially facilitate optimization of a biomechanical intervention for treating musculoskeletal disuse.

TABLE OF CONTENTS

LIST OF FIGURES

LIST OF TABLES

CHAPTER 1: INTRODUCTION

The musculoskeletal system is highly dynamic and has the capacity to accommodate changes in demand with respect to its mechanical environment. Both skeletal muscle and bone show the ability to change its physiologic and biochemical characteristics to adapt to new functional requirements (Salmons and Henriksson 1981; Frost 1982). Debilitating reversible or irreversible adaptations can result from disuse or reduced weight bearing, as experienced in microgravity, immobilization, bed rest, aging, and spinal cord injuries (Giangregorio and McCartney 2006). Decreased metabolic demand affects the mechanical and morphological musculoskeletal properties. Potential countermeasures include pharmaceutical agents and/or physical stimuli. While drugs are not site-specific and target a single body system, physical or mechanical regimes may benefit the combined musculoskeletal system (Shackelford, LeBlanc et al. 2004). Interventions that can mechanically load the bone in the absence of weight bearing offer a way to enhance osteogenesis during unloading/disuse conditions. The inter-relationship between bone loss and muscle atrophy suggest that an intervention must simultaneously target these two systems.

MUSCULOSKELETAL PHYSIOLOGY

The skeletal and muscular systems complement each other to provide form, stability, and movement to the body. The primary function of the skeleton is to transmit forces from one part of the body to another and to protect organs, while skeletal muscle provides strength and protection to the skeleton by distributing loads and absorbing shock (Martin, Burr et al. 1998; Nordin and Frankel 2001).

Bone Biology

Bone is a specialized composite tissue that serves diverse mechanical functions and protective roles. The bone composition includes an organic extracellular matrix of fiber and ground substance produced by cells, as well as a high content of inorganic materials such as mineral salts that combine intimately with the organic matrix (Buckwalter, Glimcher et al. 1996). The mineral portion of bone is mostly calcium and phosphate, in the form of hydroxyapatite crystals. Bone serves as a reservoir for the body's essential minerals that are embedded in network of collagen fibers. Glucosaminoglycans surround fibers and serve as cementing substance between layers of mineralized collagen fibers (Nordin and Frankel 2001).

Bone cells are embedded in a highly vascular, mineralized, osteoid matrix, among many different tissues including cartilage, nerve, fibrous tissue, marrow, adipose, and vascular. As reflected in the varied bone microstructure, mechanical functions of the bone extend beyond maintaining basic strength and stiffness, and include mechanisms to avoid fatigue fracture due to repeated loading. The long bone is enclosed within an envelope of two membranes, periosteum and endosteum, and this system of membranes isolates bone interstitial fluid from plasma (Gamble 1988).

Structure is a mixture of cortical and trabecular tissue which are identical tissue but with different morphology. Cortical and trabecular are both lamellar bone but cortical tissue is haversian lamellar bone where the haversian system or osteon makes up the functional unit of cortical bone. Each osteon represents concentric lamellae around a central haversian canal which form a network of blood vessels and nerves that nourish the bone (Cooper, Milgram et al. 1966; Gamble 1988). Within the concentric lamellae,

osteocytes are situated in separate lacunae with multiple cytoplasmic extensions running through canaliculi. These channels permit communication to other osteocytes and a passage of nutrients for metabolic exchange and ion transport between bone, extracellular fluid, and blood (Frost 1963a).

The blood supply of the bone enters a typical long bone through four distinct systems: nutrient artery, metaphyseal arteries, epiphyseal arteries, and periosteal arteries. Arterial flow is centrifugal, from endosteal surface to the periosteal surface and venous flow is the opposite. The nutrient artery enters the cortical shaft obliquely. Inside the medullary cavity, it divides into ascending and descending branches. Capillaries enter haversian canals through numerous openings to facilitate irrigation of canaliculi. At the external surface, the cortical vessels connect with the periosteal network of vessels, which join with the capillaries in the overlying muscles (Gamble 1988).

Bone Biomechanics

Bone as a composite material with two phases is stronger than either type of material alone (Bassett 1965). Strength and stiffness are important, and can be understood by examining its behavior under loading. The failure load, deformation, and energy stored before failure are reflected in the load-deformation curve. During loading in a given direction, bone will develop stress, or force per unit area, and strain, the deformation or change in bone's dimensions, in response to the externally applied load. The stiffness or modulus of elasticity, is represented by he slope of the curve in the elastic region (Turner and Burr 1993; Nordin and Frankel 2001).

Bone is an anisotropic material and exhibits different mechanical properties when loading in different directions (Martin, Burr et al. 1998). Forces can be applied to bone

structure in various directions producing tension, compression, bending, shear, or torsion. Clinically, bone is subjected to all of these loading modes. Fractures in trabecular bone are often produced by tensile or shear stresses, whereas compressive loading is commonly experience by vertebra. Fractures due to bending are common in long bones, where the bone is subjected to a combination of tension and compression (Nordin and Frankel 2001). Thus, assessment of skeletal mechanical properties has clinical relevance in evaluation of potential countermeasures.

Muscular Physiology

Skeletal muscle is the most abundant tissue in the human body (Nordin and Frankel 2001). It is a highly plastic tissue with the ability to adapt to the level of use imposed upon it (Lieber 1988; Allen, Roy et al. 1999). Skeletal muscle structure is highly organized, with the single muscle fiber as its basic structural unit. Each fiber is composed of myofibrils arranged in parallel, and are enclosed by the sarcolemma, a delicate plasma membrane. Myofibrils are the contractile elements, made up of sarcomeres, functional unit of force generation. Sarcomeres contain actin and myosin filaments, along with regulatory proteins to modulate the force generated by the muscle (Squire 1981). The endomysium surrounds individual fibers, which form bundles, or fascicles, encompassed by the perimysium. The muscle is composed of several fascicles enclosed by a fascia of fibrous connective tissue or the epimysium. The forces produced by muscle contractions are transmitted to the bone through these connective tissues and tendons that attach muscle to bone (Kasser 1996).

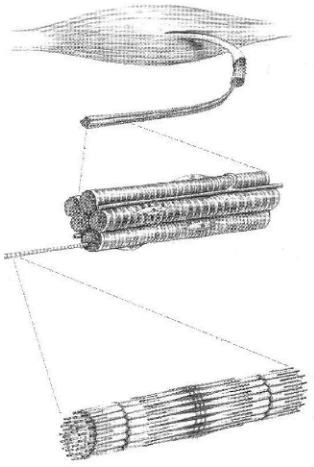

Figure 1. Muscle fiber structure. (Lieber 1986)

Myofilaments are activated by the process of excitation–contraction coupling, where, upon nerve depolarization, the action potential is transmitted to the muscle fiber at the neuromuscular junction (Ebashi 1976). Depolarization is conducted across the sarcolemma and contraction is initiated as the sarcoplasmic reticulum releases calcium. The force of contraction is developed by the myosin heads as the actin and myosin filaments move past one another to actively shorten the sarcomere.

While muscle architecture influences whole muscle contractile properties, there exists a hierarchy of functional muscle fiber properties that contribute to the rate of contraction, tension development, and susceptibility to fatigue. Fibers can be classified into three types with respect to the contractile and metabolic properties. The metabolic properties represent the pathways and rates of energy production required for calcium flow, which in turn determine contraction speed. Type I fibers are slow twitch with oxidative enzymes, and have large amounts of mitochondria. These fibers are generally smaller in diameter, and thus generate lower peak forces. There is high capillary blood flow around them to maintain high rates of oxygen and nutrient delivery. Thus, type I fibers have lower fatigability. Type II fibers are divided into two subgroups. Type IIA fibers are fast twitch oxidative-glycolytic, i.e. capacity for both aerobic and anaerobic activity. These fibers are quick to contract but fibers are mostly at rest and are activated for brief bouts of intense activity. Type IIA fibers have a well developed blood supply but fatigue at an intermediate rate. Type IIB fibers are fast twitch glycolytic and rely on anaerobic activity for ATP production. Only a few capillaries are near type IIB fibers, and thus they are not as fatigue resistant as type I and type IIA. Type IIB fibers have large diameters and thus can generate great tension, but cannot maintain the tension without rest. The extrinsic

muscle properties such as the maximum tetanic force that can be generated is determined by the physiologic cross sectional area (CSA), mass, or number of fibers (Lieber 1986).

During muscle contractions, there is a preferential fiber recruitment based on fiber properties. Type I fibers are regularly activated, and as the muscle force increases, stimulation frequency increases (Nordin and Frankel 2001). At higher levels of tension, the fast fibers with larger motor units are activated intermittently, first with recruitment of type IIA followed by type IIB. Fast fibers are more difficult to train because they are last to be activated (Lieber 1986).

Mechanics of Muscle Contraction

Tetany occurs when individual muscle twitch responses cannot be distinguished and thus the response form maximum shortening of the stimulated fiber. The frequency tension relation in human is such that slow twitches occur at around 5 Hz, unfused tetanus occurs at 10 Hz, with fused tetanus at 100 Hz (Widmaier, Raff et al. 2004). The contraction of a muscle does not necessarily imply that the muscle shortens; it only means that tension has been generated. Muscles can experience isometric contraction, in which no movement takes place, because the load on the muscle exceeds the tension generated by the contracting muscle. An isotonic contraction occurs when movement *does* take place, because the tension generated by the contracting muscle exceeds the load on the muscle. Finally, isotonic contractions are divided into two types: concentric contraction in which the muscle decreases in length (shortens) against an opposing load, or an eccentric contraction in which the muscle increases in length (lengthens) as it resists a load.

MUSCULOSKELETAL DISUSE

Musculoskeletal degeneration upon spaceflight, bedrest, aging, and spinal cord injuries causes severe changes in muscle activity and mechanical loading, causing bone loss and muscle atrophy (Giangregorio and McCartney 2006). Adaptation to disuse induces macro-structural alterations in morphology and mass, and also at the cellular and molecular levels, inducing micro-structural variations. The spectrum of disuse can range from minimal losses induced by reduced activity, to more severe de-conditioning induced by bedrest and microgravity, and finally, to extreme cases of immobilization upon spinal cord injuries (Bloomfield 1997). Several models of musculoskeletal disuse have been developed for clinical and animal studies, including unilateral limb suspension, casting immobilization, and rodent hind limb suspension.

Disuse Osteopenia

Reduced weight bearing causes severe bone loss, with increased bone resorption and decreased bone mineral density. Alterations in bone structure include increased trabecular spacing, decreased cortical thickness due to endosteal resorption, and decreases in cross sectional moment of inertia (Modlesky, Slade et al. 2005). Upon spinal cord injuries, bone loss is substantial, and the rate of bone loss is rapid and linear. Bone loss post-injury may not plateau, rather, significant amounts of loss are observed many years after SCI, but this time course may be site-specific (Eser, Frotzler et al. 2004). Trabecular bone changes level off within 1-3 years of immobilization, but cortical loss can progressively decrease beyond 10 years post-injury (Zehnder, Luthi et al. 2004). Changes are also site specific to lower limbs, usually at the distal femur, proximal tibia trabeculae, and tibial/femoral diaphyses, with up 20% trabecular loss, 3% to 4% cortical loss (Frey-

Rindova, de Bruin et al. 2000). Upon paralysis of the lower limb, bone density of femoral neck and proximal tibia decreased by 65% and 45%, respectively (Biering-Sorensen, Bohr et al. 1990). A clinical study that subjected healthy males to 120 days of bedrest showed a 51% increase in bone resorption (Vico, Chappard et al. 1987). Animal studies have shown decreased trabecular bone mass and periosteal bone formation rates upon spaceflight (Jee, Wronski et al. 1983; Wronski and Morey 1983). The risk of fracture increases with prolonged exposure to disuse conditioning, and common fracture sites include distal femur or proximal tibia.

Muscle Atrophy

Muscle atrophy induced by disuse conditioning is just as severe as bone loss, but may be very important because muscle atrophy precedes bone loss (Giangregorio and McCartney 2006). Muscular atrophy has been characterized in many human models including microgravity, unilateral lower limb suspension, bedrest, and spinal cord injuries. Exposure to microgravity has shown to decrease muscle mass, force, power, and increase fatiguability (Pavy-Le Traon, Heer et al. 2007). Four weeks of unilateral lower limb suspension showed 7% decrease in mid-thigh muscle CSA, and after 6 weeks, fiber CSA decreased by 14% (Tesch, Berg et al. 1991). Within 6 weeks of spinal cord injuries, average muscle cross sectional areas (CSAs) decreased by 18% to 46% (Castro, Apple et al. 1999), and after one year, lean mass was reduced by 15% (Wilmet, Ismail et al. 1995). Increasing age and duration of injury are associated with further loss of lean mass.

In addition to morphological alterations, there are severe changes in muscular mechanical properties. Bedrest has shown a 20% decrease muscle strength and peak torque of knee extensor muscles (Dudley, Duvoisin et al. 1989) and decreased maximum

isometric tension (LeBlanc, Marsh et al. 1985). The slow twitch, type I fibers usually exerts a smaller force over longer periods of time and maintains posture where as the fast twitch, type II fibers are more involved in locomotion (LeBlanc, Marsh et al. 1985). Muscle fibers shift toward faster, less oxidative phenotypes after prolonged disuse (Lieber, Ferro et al. 1988). A 35-day bedrest study showed slow and fast twitch fiber CSA decreased by 8% and 15%, respectively (Bloomfield 1997).

SKELETAL ADAPTATION

Potential countermeasures of disuse osteopenia and muscle atrophy include pharmaceutical drugs and/or physical stimuli. Pharmaceutical agents are often associated with side effects that may exclude patients. In addition, these treatments are not site-specific, a factor that is important in disuse conditions because the extent of damage often depends anatomical location and condition of the disuse. The unloading environment affects several physiologic systems, including muscular and skeletal, but pharmaceutical agents may successfully target only one system. The musculoskeletal system is highly dynamic and demonstrates functional adaptability to physiological demands. An increase in demand can be generated by physical or mechanical stimulus, which has potential to simultaneously induce an adaptive response in both bone and muscle.

Bone Adaptation to Mechanical Strain

Bones has long been recognized to sense the mechanical loads they bear, and self-regulate, and modify their structures to suit changes in these loads (Wolff 1892). Although mechanical adaptability has implications for disuse osteoporosis during unloading, understanding this natural phenomenon is essential for designing a biomechanically based intervention. Experimental models of skeletal loading have been

developed to investigate the structural changes and potential underlying mechanisms of adaptation.

Deformations, or bone strains, have been shown to influence the initiation and control of bone adaptation to mechanical loading (Koch 1917; Thompson 1917). Responses to deformations have been demonstrated at the cellular level in tissue culture (Glucksmann 1938), and also at the bone architectural level with the application of strain gauges to bone *in vivo* (Lanyon and Smith 1969). The "mechanostat" theory suggests that strains must be maintained within a range to induce a response. Beyond a threshold, bone mass and bone strength will increase, but if strain remains below threshold, remodeling is enhanced which results in a negative bone balance (Frost 1990).

Measurement of strain in living animals has demonstrated the role of strain magnitude on bone response (Lanyon 1973; Lanyon 1974; Lanyon, Hampson et al. 1975). In addition to strain magnitude, the role of several strain-related factors has been investigated by creating a controlled strain environment *in vivo*. A functionally isolated avian ulna model showed that strains above 1000 με increased osteogenic activity, suggesting that adaptive remodeling is sensitive to specific strains. Strain distribution was also suggested to influence the adaptive response when new bone formation was observed although experimental loads were applied at or below normal physiologic strains (Rubin and Lanyon 1985). Experiments of applied loading in the forearms of adult sheep (O'Connor, Lanyon et al. 1982) and to the ulna of growing rats (Mosley and Lanyon 1998) have demonstrated osteogenesis at higher strain rates, and impact exercises associated with high strain rates have been correlated with increased bone formation rates (Judex and Zernicke 2000).

Anabolic Potential of Dynamic Loads

The anabolic responses observed during intermittent loading has emphasized the importance of dynamic loads (Martin and Burr 1989). Continuous bending of the rabbit tibia suppressed periosteal apposition and showed no effect on endosteal bone formation (Hert, Liskova et al. 1969). However, dynamic loading on the same model increased periosteal and endocortical bone formation (Liskova and Hert 1971). Static loads applied to the avian ulna demonstrated changes that are observed during immobilization, with increased endosteal resorption and increased intracortical porosity, whereas the dynamic loads increased net bone formation (Rubin and Lanyon 1984). A rat ulna loading model showed that static loads did affect appositional bone formation but dynamic loading enhanced osteogenesis at both periosteal and endocortical surfaces (Robling, Duijvelaar et al. 2001).

These studies indicate that bone is anabolic to dynamic stimuli, suggesting that parameters such as cycle number and loading frequency are critical factors that influence bone's adaptive response. Compressive loads applied at a frequency of 0.5 Hz with only 36 cycles per day was shown to enhance bone mineral content, sub-periosteal and endosteal new bone formation, demonstrating that only a short exposure to loading is required to induce an anabolic response (Rubin and Lanyon 1984). Studies have also shown that high frequency loads require lower orders of strain to induce an anabolic response (Qin, Rubin et al. 1998). Ten minutes of high frequency but low magnitude mechanical signals have demonstrated the ability to prevent bone loss in conditions of microgravity (Rubin, Xu et al. 2001).

Mechanotransduction via Bone Fluid Flow

Many loading parameters influence the anabolic potential of dynamic mechanical stimuli, however, the event that mostly likely influences bone cell behavior is a consequential parameter of strain itself (Rubin and Lanyon 1985). As previously discussed, bone is a composite material of complex structure with a network of lacunar-canalicular channels with cytoplasmic extensions that allows osteocyte communication and nutrient passage for metabolic exchange. The intricate structure comprised of lacunae-canaliculi channels permit interstitial fluid flow through tiny microporosites. (Weinbaum, Cowin et al. 1994; Cowin, Weinbaum et al. 1995). Early studies suggested that loading-derived flow through canaliculi was used to enhance nutrient and waste product transport between osteocytes (Piekarski and Munro 1977). However, more recent theories on mechanostransduction propose load induced fluid flow through bone interstices as biophysical signal in mechanotransduction that can actually inform the cells about their mechanical environment (Weinbaum, Cowin et al. 1994).

Theoretical and experimental data have shown show that bone cells are sensitive to load induced fluid flow and the physical/mechanical signal could be translated to the cell by "by products" of load such as change in fluid velocities or pressure (Reich, Gay et al. 1990; Weinbaum, Cowin et al. 1994; Jacobs, Yellowley et al. 1998; Burger and Klein-Nulend 1999). It has been proposed that instead of the bulk strain that results from loading the whole piece of bone, a local force resulting from that strain acts on the bone cells. The local force can be derived from the displacement of fluid in the canaliculi (Weinbaum, Cowin et al. 1994).

Studies have linked anabolic potential of dynamic loading to the role of bone fluid flow, implying fluid movement cannot be caused by static load, rather, that cyclic loading

and relaxation is required to move fluid through bone. Optimizing mechanical parameters such as loading frequency, cycle number, and strain rate is essential for regulation fluid excitations. Fluid flow dependency on loading frequency has been demonstrated (Qin, Rubin et al. 1998), consistent with reports of the anabolic potential of high frequency loads (Rubin, Turner et al. 2002). Varying the frequency of cyclic compressive load applied to the rat ulna suggested that the viscoelasticity of the cell or extracellular matrix will affect the amount of cellular deformation resulting from fluid forces (Hsieh and Turner 2001). Thus, higher loading frequencies, with higher strain rates, could cause rapid local fluid movements and that might initiate cellular events faster.

Intramedullary Pressure Gradients

It has been hypothesized that bone interstitial fluid flow induced by changes in intramedullary pressure (ImP) can influence bone remodeling (Reich, Gay et al. 1990). Several studies have demonstrated that such ImP gradients generated during loading can regulate intracortical fluid flow (Qin, Lin et al. 2002). Bone remodeling has been shown in various *in vivo* models in which intramedullary pressures (ImP) were elevated via venous occlusion (Kelly and Bronk 1990). A hind limb suspension rat model subjected to venous ligation showed adaptive response as indicated by increase in bone mineral content, trabecular density, length, and distal width of femurs, independent of loading induced mechanical strain (Bergula, Huang et al. 1999). A functionally isolated avian ulna model was used to demonstrate the anabolic response of fluid pressure oscillations. In this experiment, a short duration of high frequency loading resulted periosteal and endosteal bone formation (Qin, Kaplan et al. 2003).

It has recently been hypothesized that the skeletal muscle pump can enhance fluid flow through the bone matrix (Winet 2003). Skeletal muscle contractions can alter blood circulation adjacent to bone, and enhance blood pressure via temporary occlusion of arteries and veins. The generated pressure waves have been suggested to increase hydraulic pressure in cortical bone capillaries and result in amplified capillary filtration. Thus, muscle dynamics may present a non-invasive mechanism of inducing changes in ImP.

As previously discussed, bone's anabolic potential upon dynamic loading are influenced by several mechanical parameters. However, the role of muscle dynamics on bone adaptation is unclear. As muscular adaptation to physiologic stimuli has been well documented, potential advantages of utilizing the muscular system to enhance ImP and subsequently influence the skeletal anabolic response are immense. The design of therapeutic regimes to simultaneously target the muscular and skeletal systems required a thorough understanding of the physiologic adaptations of each individual system. Similar to reports on bone's specificity to particular loading regimes and dependence on mechanical parameters, studies on muscular stimulations have demonstrated a wide range of adaptive responses.

MUSCULAR ADAPTATION

The motivations for developing muscular therapies are enormous, given the devastating consequences of physiological disuse. Muscle is a highly plastic tissue, and muscle strength, mass, and volume are well known to increase with training (Gonyea,

Ericson et al. 1977). An increase in demand can be generated by exercise or electrical stimulation (Salmons and Henriksson 1981). Training via isometric strengthening can increase fiber CSA, the number of slow twitch fibers, and the rate of muscle protein synthesis (Giangregorio and McCartney 2006).

Parameters of Electrical Stimulation

Electrical stimulation is well established (Delitto and Snyder-Mackler 1990) for enhancing muscle performance. There are several critical parameters that must be considered in design muscle stimulation regimes. In therapeutic clinics, the objective of the treatment is often determined by the variations stimulation protocols. A few of these parameters include waveform type, intensity, duration, duty cycle, period, and cycle number (Graupe 2002). Rectangular waveforms are often used because the shape is directly related to the excitability of nerve tissue, and the high rate of rise increases the current's ability to induce excitation. Higher intensities permit stimulation of fibers with higher thresholds and those located deeper in the tissue (Prentice 2002). Longer durations allow more fibers to react to the stimulus and lower intensities. The duty cycle representing on to off ratio of current flow is designed to mimic voluntary contraction and relaxation phases of normal physiologic exercise (Cameron 2003). The length of the pulse period determines the mechanism of stimulation. Short pulses stimulate nerve fibers whereas longer pulses are used to induce contractions in denervated muscle. Pulse periods less than 1 ms usually minimize pain. The number of cycles, or frequency, determines the amount of muscle shortening and recovery. As the number of twitch per second increases, a summation of contractions occurs in which single twitches cannot be distinguished, and tetanization is reached (Widmaier, Raff et al. 2004). Muscle fibers

usually develop greater magnitudes of tension in tetany, thus, high frequency is applied for enhancing muscle tension.

Experimental Applications of Muscle Stimulations

While voluntary contractions demonstrate preferential and asynchronous fiber recruitment, electrical stimulations induce a more synchronous firing of motor units, and order of fiber recruitment is reversed. While voluntary contractions first activate slow twitch fibers, electrical stimulation first recruits fast twitch fibers (Sinacore, Delitto et al. 1990). Although more simultaneous activations may improve muscle strength, it can also cause early fatigue, necessitating rest or recovery periods between pulses (Prentice 2002).

Electrical stimulation (ES) has been applied to spinal cord injury patients, to produce isometric contractions. Results indicated increased lower extremity muscle volume by 10% and a 22% increase with more frequent bouts (Skold, Lonn et al. 2002). Muscle CSA, maximal force generated, and fatigue resistance were also enhanced (Baldi, Jackson et al. 1998).

The effects of chronic low frequency stimulation were compared with the effects of exercise and results showed that the forms of increased use share the same basic mechanism of adaptation (Salmons and Henriksson 1981). Exercise represents only an intermittent stimulus to muscle because motor units are recruited in a more selective fashion, whereas during stimulation, all of the fibers participate and changes are synchronous. Thus electrical stimulation is able to achieve complete transformation of fiber type and reveals the full adaptive capacity of muscle tissue. These changes include, but are not limited to, fast to slow fiber transformation, increased capillary density, and increased resistance to fatigue. Muscle strengthening depends on the stress imposed on

the muscle, and thus, in addition to bulk mass, muscle fiber CSA and force generating capacity are critical endpoints to evaluate (Lieber 1988).

Several studies have compared low and high frequency stimulation and its ability to prevent muscle atrophy. One study showed that lower, unphysiologic frequencies for longer durations were more effective than high frequency stimulations in preventing muscle atrophy (Dupont Salter, Richmond et al. 2003). However, many studies have demonstrated the effectiveness of short duration, high frequency stimulations. Whereas slow fibers are physiologically activated at low frequencies, fast fibers may be activated only intermittently with high frequency bursts of electrical activity. A rat immobilization model showed that gastrocnemius stimulations at 50 Hz frequency, 10 minutes per day, for 10 days normalized type II fiber CSA to control values and restored mechanical properties (Mattiello-Sverzut, Carvalho et al. 2006). This frequency range was selected to re-establish muscle's force generating ability because it preferentially recruits type II fibers (Delitto and Snyder-Mackler 1990; Sinacore, Delitto et al. 1990). Similarly, stimulation of the immobilized rabbit tibialis anterior at 50 Hz effectively minimized reduction of muscle fiber cross sectional area (Qin, Appell et al. 1997). Finally, brief periods of stimulation of rat gastrocnemius at 100 Hz, with 5 minute recovery periods were shown to be effective inactivity induced muscle atrophy (Kim, Roy et al. 2007).

Combined Musculoskeletal Potential of Muscle Dynamics

Few studies have investigated to role of muscle dynamics as a loading regime for bone adaptation. One study demonstrated an increase in mechanical strength upon muscle contractions stimulated via ischiatic nerve (Nordsletten, Kaastad et al. 1994). A

rat hind limb suspension model demonstrated enhanced tibial trabecular bone formation upon chronic electrical stimulation at a 10 Hz frequency (Zerath, Canon et al. 1995). Another study used a similar animal model to evaluate the role of a range of frequencies from 1 Hz to 50 Hz. The results from this study indicated that high frequency stimulation are more osteogenic, since bones experience a greater load application (Wei, Ohira et al. 1998). In a similar model, the magnitude of peak compressive strains induced by 30 Hz muscle contractions were measured, and this stimulation was further shown to reduce the extent of osteopenia (Midura, Dillman et al. 2005). A clinical study of spinal cord injury patients demonstrated partial reversal of disuse osteopenia and recovery of muscular strength upon electrical stimulation (Belanger, Stein et al. 2000). Although the role of strain-related parameters on bone's anabolic response offers insight in design optimal loading regimes, it is unclear whether muscle dynamics can be applied for simultaneous muscular therapy.

CHAPTER 2: HYPOTHESIS AND SPECIFIC AIMS

The inter-relationship between bone loss and muscle atrophy is essential since both physiologic systems are severely affected by disuse conditioning. Currently no exercise or mechanical loading intervention has shown consistent prevention or reversal of bone loss and muscle atrophy (Giangregorio and McCartney 2006). Muscle morphology and strength has been shown to recover at a faster rate than bone, however, the imbalance in bone and muscle strength increases the risk of fracture (Bloomfield 1997). If muscle atrophy can be minimized during prolonged bed rest, bone loss may be diminished (Bloomfield 1997). Therefore there is a need for understanding the usefulness of active muscle contraction to simultaneously treat the musculoskeletal system.

It has recently been hypothesized that muscle dynamics influence the bone interstitial fluid flow and thus induce bone adaptation (Winet 2003). The regulatory role of bone intramedullary pressure (ImP) on bone fluid flow, and consequently, bone adaptation, has been shown effective (Qin, Kaplan et al. 2003). Thus it has been suggested that muscle contraction can induce such fluid flow and enhance perfusion via hypertension of the microvasculature, and affect modulation of ImP, potentially mediating bone adaptation. Thus muscle stimulations can be applied as a form of mechanical loading to the bone, with potentials to induce both a muscular and a skeletal response. Strain-related parameters greatly influence the musculoskeletal response, as studies have demonstrated that application of short duration, high frequency dynamic loads can induce substantial adaptation, enhance osteogenesis, and potentially prevent disuse induced bone loss (Rubin and Lanyon 1984; Rubin, Xu et al. 2001). The parameters associated with an optimal response in muscle dynamics are unclear for simultaneous treatment of two

physiologic systems. **Therefore, the overall hypothesis of this study is that low magnitude, short duration, and high frequency dynamic muscle contractions can regulate mechanotransductive conditions and have therapeutic potentials to prevent bone loss and muscle atrophy induced during functional disuse.** Muscle dynamics has been shown to enhance ImP in a rat disuse model and thus induce a skeletal adaptive response. However, determining the optimal loading parameters required to induce such a response is important as reports of muscle stimulation on bone response are inconsistent (Giangregorio and McCartney 2006). Evaluating the role of critical parameters like frequency specificity and optimal recovery periods across species is necessary for safe and effective clinical therapeutic design. This study will determine the therapeutic potential of muscle dynamics in a disuse mouse model. The mouse model can be further extended to assess molecular and genetic mechanisms of such a biomechanical intervention. The overall hypothesis of this study will be tested with two specific aims that address the role of frequency and recovery periods during dynamic muscle stimulation in a disuse mouse model.

SPECIFIC AIM 1. Evaluate frequency specificity in the range between 1 Hz and 50 Hz of dynamic muscle contractions on bone and muscle adaptation.

Sub-Hypothesis 1. Dynamic muscle stimulations will influence musculoskeletal adaptation in the disuse environment in the high frequency range by demonstrating attenuation of bone morphology, bone strength, and muscle morphology.

Sub-Specific Aim 1.1. Evaluate adaptations in trabecular and cortical morphology upon administration of muscle stimulation treatment in a functional disuse environment.

Sub-Specific Aim 1.2. Evaluate the extent of attenuation in skeletal mechanical properties upon muscle stimulation treatment during exposure to disuse.

Sub-Specific Aim 1.3. Evaluate extent of attenuation in muscle wet weight and muscle fiber cross sectional area upon muscle stimulation treatment during exposure to disuse.

SPECIFIC AIM 2. Evaluate the role of a short-term recovery period during dynamic muscle contractions on bone and muscle adaptation.

Sub-Hypothesis 2. Dynamic muscle stimulations with insertion of a short-term recovery period will enhance the adaptive response in bone morphology, strength, and muscle morphology.

Sub-Specific Aim 2.1. Evaluate adaptations in trabecular and cortical morphology upon administration of muscle stimulation treatment with short-term rest insertions.

Sub-Specific Aim 2.2. Evaluate the changes in skeletal mechanical properties upon muscle stimulation treatment with short-term rest insertions.

Sub-Specific Aim 2.3. Evaluate changes in muscle wet weight and muscle fiber cross sectional area upon muscle stimulation treatment with short-term rest insertions.

CHAPTER 3: FREQUENCY SPECIFICITY OF DYNAMIC MUSCLE CONTRACTIONS

ABSTRACT

Skeletal muscle dynamics have been suggested as a modulator of intramedullary pressure, generating mechanotransductive signals that may play a role in bone adaptation. The objective of this study was to evaluate the role of frequency variations of dynamic muscle contractions at 1 Hz, 20 Hz, 30 Hz, and 50 Hz as a potential therapeutic to prevent bone loss and muscle atrophy in a disuse mouse model. Fifty-two BALB/c mice were randomized into 7 groups: baseline control, age-matched control, hind limb suspension non-stimulated (HLS-NS), and HLS with muscle contractions at 1 Hz, 20 Hz, 30 Hz, and 50 Hz. Micro-CT analysis showed reduction in trabecular (-19% to -62%, $p<0.01$) and cortical (-8% to -15%, $p<0.01$) bone morphology parameters, as well as mechanical strength parameters such as bone tissue stiffness (-21%, $p<0.01$) and ultimate strength (-19%, $p<0.01$) as demonstrated by a four-point bending test. Hind limb suspension also significantly reduced hind limb muscle weights (-15% to -26%, $p<0.05$) and fiber cross sectional area (CSA) (-48%, $p<0.001$). Muscle stimulations demonstrated significant attenuation of trabecular bone volume fraction at 1 Hz (+34%, $p<0.05$), 20 Hz (+47%, $p<0.01$), 30 Hz (+27%, $p<0.05$), and 50 Hz (+48%, $p<0.01$). Cortical area also showed increasing trends upon muscle stimulation at 1 Hz (+6%, $p<0.05$), 20 Hz (+7%, $p<0.05$), 30 Hz (+8%, $p<0.05$), and 50 Hz (+10%, $p<0.01$). Mechanical properties of the bone were enhanced when compared with hind limb suspension control, demonstrated by attenuation of tissue stiffness at 1 Hz (+6%), 20 Hz (+17%, $p<0.05$), 30 Hz (+15%), and 50 Hz (+13%) and maximal force at 1 Hz (+11%), 20 Hz (+23%), 30 Hz (+11%), and 50 Hz (+28%, $p<0.05$). Stimulations at 30 Hz enhanced cortical geometry but trabecular

bone was unaffected. Muscle fiber CSA was attenuated upon muscle stimulations at 1 Hz (+13%), 20 Hz (+38%), 30 Hz (+45%, $p<0.05$), and 50 Hz (+31%). Among all signals, the high frequency range generated significant attenuation in muscle and bone, suggesting the 20 Hz to 50 Hz frequencies as an optimal range for noninvasive prevention of bone loss and muscle atrophy.

INTRODUCTION

The highly dynamic and adaptive nature of the musculoskeletal system has devastating implications during exposure to the disuse environment. The severe adaptive responses experienced by astronauts, bedrest and spinal cord injury patients include alterations in morphological and mechanical properties of both muscle and bone. Pharmaceutical treatments have been shown to target either muscle or bone, however, these agents have side effects, are not site specific, and cannot simultaneously treat both skeletal and muscular systems. Mechanical loading regimes have long been shown to induce adaptive response in both muscle and bone, and designing such treatment may offer an intervention that is non invasive and can easily be applied during disuse de-conditioning. Skeletal loading studies have shown that low magnitude, high frequency loading is osteogenic, and only a short duration of stimulation is required to induce such a response. The inter-relationship between muscle and bone may be essential for a simultaneous treatment. Studies of muscle adaptation have suggested positive effects of both chronic, low frequency and short-term, high frequency stimulations. Such a form of mechanical loading on both muscle and bone can be induced by muscle contractions. It has been suggested that fluid pressure gradients generated during muscle contractions may be influence bone's adaptive response. Muscle loading regime parameters optimal for both muscle and bone are unclear; therefore, the objective of this study is to evaluate the adaptive role of frequency specificity of dynamic muscle contractions in a functional disuse model as a preventive treatment of musculoskeletal disuse. It is thus hypothesized that an adaptive response will be observed in trabecular and cortical bone morphology, bone mechanical strength, and muscle mass and fiber morphology.

MATERIALS AND METHODS

Animal Model

Several models of functional disuse have been utilized including immobilization via plaster casting or nerve resection, however, the hind limb suspension model has been widely used because it closely mimics spaceflight conditions in which limbs are not load bearing but are still mobile (LeBlanc, Marsh et al. 1985; Morey-Holton and Globus 2002). The BALB/cByJ (BALB) mouse strain was selected for this study because of the response in bone morphology and bone formation rates upon unloading and mechanical stimulation (Judex, Donahue et al. 2002; Judex, Garman et al. 2004). When compared to C57BL/6J and C3H/HeJ strains, BALB mice show the greatest disuse induced trabecular bone loss, and strongest change in bone formation rates upon mechanical stimulation (Judex, Donahue et al. 2002). Fifty-two adult female BALB mice were randomized by weight into 7 groups: baseline control, age-matched control, hind limb suspension non-stimulated (HLS-NS), or HLS with stimulated muscle contractions at 1 Hz, 20 Hz, 30 Hz, and 50 Hz (Table 2). All animals were 5.5 months of age at the start of the experiment and animals were subjected to unloading and/or stimulation for 21 days.

Table 2. Experimental design.

Group	N
Baseline Control	6
Age-Matched Control	6
HLS	8
HLS + 1hz	8
HLS + 20Hz	8
HLS + 30z	8
HLS + 50z	8

Procedures for unloading were adapted from previous hind-limb unloading rodent models (Morey-Holton and Globus 2002; Squire, Brazin et al. 2007). Animals were anesthetized using 2% inhalant isoflurane to restrain each mouse during the suspension preparation. Hind limbs of animals were elevated using a swivel hook apparatus to allow the animal to rotate freely. Tincture of benzoin was applied along the length of the tail as an adhesive and allowed to dry for a few minutes. A strip of tape was attached to a plastic tab through a paperclip loop and the fishline swivel was connected to the paperclip. The length of tail was taped along both sides and another piece of tape was applied in a circular fashion to secure the apparatus. The fishline swivel was attached to a plastic rod (Polyvinyl chloride type I rod, McMaster-Carr, Dayton, NJ). Two holes of 0.25 inch diameter were drilled at the end of each cage to hold the rod, suspension apparatus, and animal. This setup allows 360° rotation and movement along the length of the rod attached inside the cage, using only the forelimbs. The angle and height of each animal were check twice a day and adjusted if necessary. Animals were fed standard rodent diet, water, and provided Napa Nectar (SE Lab Group) to minimize discomfort and to prevent dehydration. Daily body weight changes were monitored, and any changes in physical appearance were recorded including temperature of the ear, color around eyes, hair loss, and reduced activity. Animals that showed a 10% decrease in body weight were fed Bacon Softees (Bioserv). Antibiotic ointments were applied if animal showed increased redness around the eyes. Veterinary technicians were consulted upon observation of severe changes. Sick animals or animals with weight loss greater than 20% were euthanized.

Signal and Stimulation

Muscle contractions were stimulated in the right quadriceps of each mouse using a Tektronix 25MHz, single channel Arbitrary/Function Generator (Exphil, Bohemia, NY). A pulse waveform was applied using the burst mode to generate a repeated signal of 1 ms pulse period, in 5 second intervals, with 2 seconds "on" and 3 seconds "off" (Figure 2). Signal amplitude of 1.2 Vpp was selected based on the observation of a strong, sustained muscle contraction for the duration of 10 minutes. A rectangular pulse waveform was selected because the shape is directly related to the excitability of nerve tissue, and a high rate of rise increases current's ability to excite nervous tissue (Prentice 2002; Cameron 2003).

Animals were prepared for stimulation by shaving both left and right hind limb fur adjacent to the quadriceps. Seirin acupuncture needles of 0.12 mm diameter (UPC Medical Supplies, Inc, San Gabriel, California) were gently inserted onto a shaved skin surface of the right quadriceps. The active, negative electrode was designated at the distal region, while the positive electrode was placed at the proximal region of the quadriceps muscles, to easily induce membrane depolarization and replicate the naturally occurring pattern of electrical flow in the body (Prentice 2002). Current was delivered to the muscle for 2 seconds, followed by a 3 second repeated rest period to mimic voluntary contraction and relaxation phases of normal physiologic exercise (Cameron 2003).

Table 3. Loading signal**.**

Frequency	Cycles
1 Hz	240
20 Hz	4,800
30Hz	7,200
50 Hz	12,000

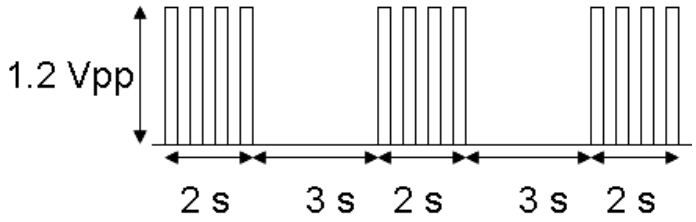

Figure 2. Repeated rest ratio of the applied muscle stimulation.

Tissue Collection and Preparation

Animals were euthanized at the end of 3 weeks of stimulation and upon sacrifice hind limb muscles including the soleus, gastrocnemius, quadriceps, were carefully dissected and weighed. Quadriceps muscles were elongated and attached to wooden rods using pins and immersed in TissueTek optimum cutting temperature mounting medium. Samples were subsequently frozen in dry-ice and liquid nitrogen cooled isopentane, and stored at -80˚C. Femurs were harvested and stored in a 50% ethanol/saline solution.

Micro-Computed Tomography

Two femoral regions were scanned using the micro-CT (Scanco Medical AG, Switzerland) at a resolution of 8 micron. A 1 mm region of the distal femur metaphysis and a 0.5 mm region of the mid-diaphysis were scanned and analyzed separately. The software provided by Scanco Medical AG was used to quantify morphology parameters of the trabecular and cortical bone.

The starting slice of metaphyseal trabecular bone analysis was identified as the point where the femoral condyles merge. This point was used as a landmark and first slice of analysis was taken 560 microns below this point. Contour lines were drawn to separate trabecular and cortical bone for a 1 mm distance. Analyzer was blinded to experimental group labels of each sample during analysis. The sigma, support, and threshold values

selected were 0.6, 1, and 320, respectively. The parameters quantified include trabecular bone volume fraction (BV/TV), connectivity density (Conn.D), trabecular number (Tb.N), trabecular thickness (Tb.Th), trabecular separation (Tb.Sp), and structural model index (SMI).

The cortical bone was analyzed at the femoral mid-diaphysis for a 0.5 mm distance. The sigma, support, and threshold values selected were 0.1, 1, and 400, respectively. The cortical morphology parameters quantified include cortical area (Ct.Ar), cortical thickness (Ct.Th), periosteal envelope (Ps.En), endocortical envelope (Ec.En), and maximum and minimum moment of inertia (Imax, Imin).

Mechanical Testing

Upon completion of scanning, femurs were preserved in –20°C with saline-soaked gauze until mechanical testing was performed. Bones were thawed for 4 hours prior to testing at room temperature in saline. A four point bending test was performed with a loading lower support span of 6 mm and upper loading span of 4 mm (Figure 3). Force was applied at a loading rate of 0.05 mm/second. The force and displacement data were normalized to obtain stress and strain data using the following equations (Turner and Burr 1993):

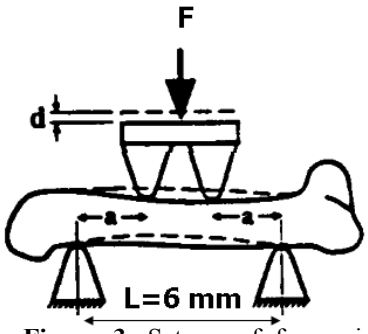

Figure 3. Set up of four-point bending test. (Turner and Burr 1993)

Stress σ = Fac / (2*I) (MP)

Strain ε = 6cd / (a(3L-4a)

Analysis of the force-displacement and stress-strain curved showed that each bone sample displayed two or more linear regions, potentially due to rigid body movement or microcracking during testing (Figure 4). Stiffness represents the slope of the force-

displacement curve, while elastic modulus represents the slope of the stress-strain curve. Stiffness and elastic modulus were computed for each individual linear region. In addition, the slope of the best fit line over all regions was computed. From these plots, the maximum and failure force/stress were determined.

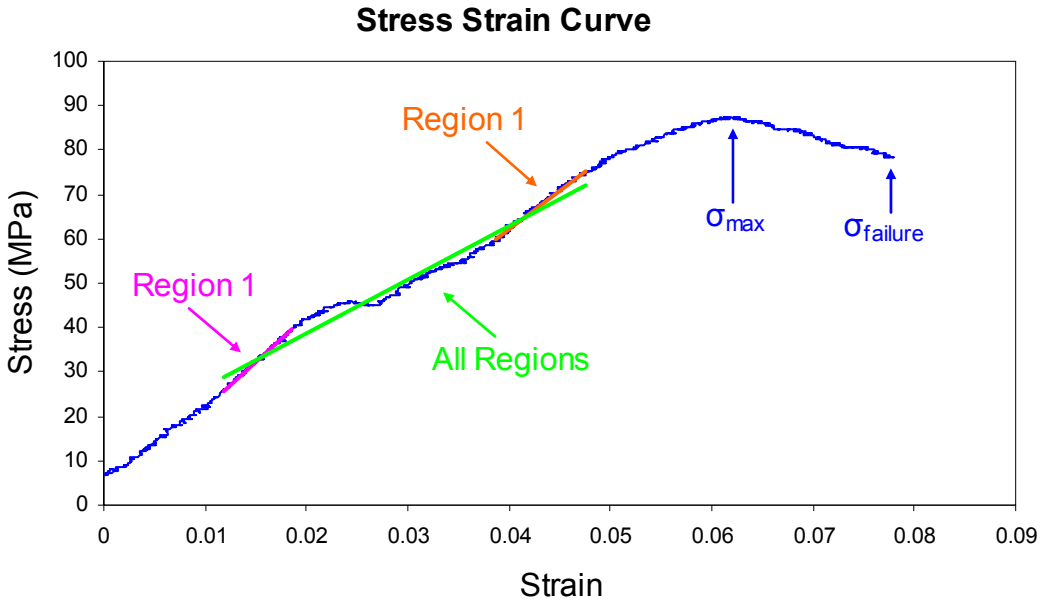

Figure 4. Stress strain cure of a control femur subjected to a four-point bending test. Elastic moduli were computed for each linear region and also for all regions using a best fit line. Maximum and failure stress were determined and compared across all frequency groups.

Muscle Histology

Frozen cross sections of quadriceps muscles were cut with a Leica cryostat microtome at 8 micron thickness, and picked up onto Colorfrost glass slides. Sections were stained with hematoxylin and eosin, and cross sectional images were captured using a digitized microscope (Zeiss, AxioVision 4, Germany) at 20X magnification. Images were uploaded into ImageJ (NIH) and cropped at the center to obtain dimensions of 650 pixels by 515 pixels at a resolution of 1.92 pixels per μm. The numbers of fibers within the cross section, excluding those touching the border, were counted. Contour lines were

drawn around each fiber, and ImageJ software was used to quantify individual fiber area. Analyzer was blinded to experimental group labels of each sample during analysis.

Statistics

All statistical tests were performed using SPSS 15.0 for Windows (Evaluation Version). For all of the analyses (micro-CT, mechanical testing, muscle mass and morphology), analysis of variance (ANOVA) with Tukey's post hoc test was used to detect differences between hind limb suspension control and all experimental groups. Significance level of 0.05 was used for all analyses.

RESULTS

Bone Morphology

Micro-CT analysis was performed for two femoral regions: distal trabecular bone and mid-diaphyseal cortical bone. Hind limb suspension induced significant changes in both trabecular and cortical bone morphology parameters. Intervention with dynamic muscle contractions demonstrated varying degrees of attenuation.

Hind limb suspension groups demonstrated significant alterations in bone volume fraction (-62%, $p<0.01$), connectivity density (-40%, $p<0.001$), trabecular number (-19%, $p<0.001$), trabecular thickness (-28%, $p<0.001$), trabecular spacing (+22%, $p<0.001$), and structural model index (SMI) (+128%, $p<0.001$) (Figure 6, 7, 8). Dynamic muscle stimulations reduced the extent of bone loss with respect to bone volume fraction (+34%, $p<0.05$; +47%, $p<0.01$; +27% $p<0.05$; +48%, $p<0.01$) at frequencies of 1 Hz, 20 Hz, 30 Hz, and 50 Hz, respectively (Figure 6). Similarly, connectivity density increased significantly from HLS control (+50%, $p<0.001$; +60%, $p<0.001$; +32% $p<0.05$; +65%, $p<0.001$) at 1 Hz, 20 Hz, 30 Hz, and 50 Hz, respectively (Figure 7). A significant difference was detected between the connectivity density of 30 Hz stimulation and 50 Hz stimulation ($p<0.05$) (Figure 7). There was also a significant reduction in the loss of trabecular number (+10%, $p<0.05$; +15%, $p<0.001$; +8% $p<0.05$; +15%, $p<0.001$) at 1 Hz, 20 Hz, 30 Hz, and 50 Hz, respectively (Figure 7). Attenuation of trabecular spacing was also observed upon stimulation at all frequencies including 1 Hz (-10%, $p<0.01$), 20 Hz (-14%, $p<0.001$), 30 Hz (-9% $p<0.05$), and 50 Hz (-14%, $p<0.001$) (Figure 7). The SMI was also altered at 1 Hz (-17%, $p<0.05$), 20 Hz (-22%, $p<0.01$), 30 Hz (-7%), and 50 Hz (-18%, $p<0.05$), indicating that the muscular intervention induced the trabeculae to

assume a more plate-like structure (Figure 8). A significant difference between 20 Hz and 30 Hz was detected in the alteration of SMI ($p<0.05$) (Figure 8). Trabecular thickness was not significantly altered by muscle stimulations at any frequency (Figure 7).

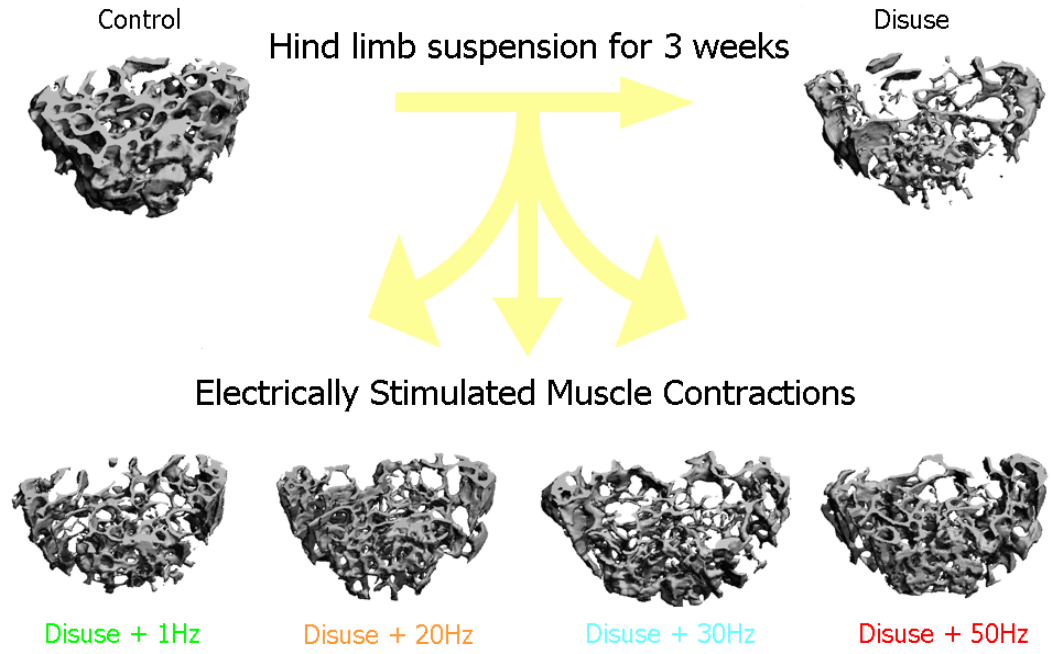

Figure 5. Three dimensional micro-computed tomographic images of trabecular bone of the distal femur upon hind limb suspension and dynamic muscle stimulations.

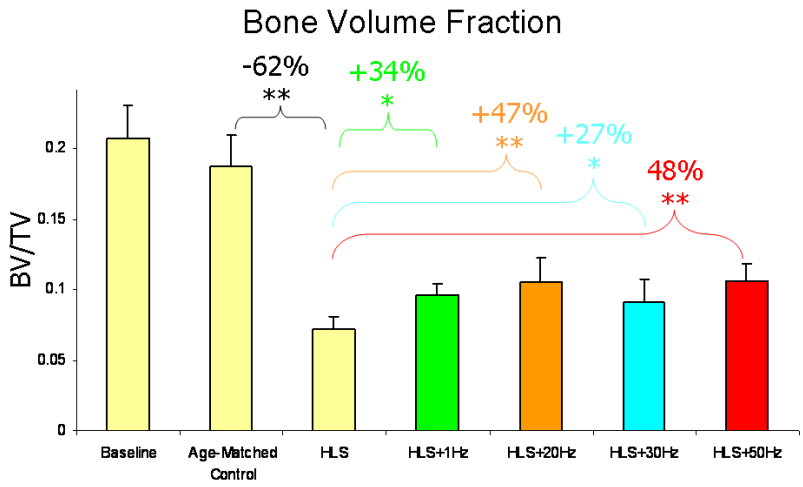

Figure 6. Bone volume fraction was reduced upon HLS, and dynamic muscle contractions demonstrated significant attenuation at each frequency, with the strongest response observed at 20 Hz and 50 Hz. (*p<0.05, **p<0.01)

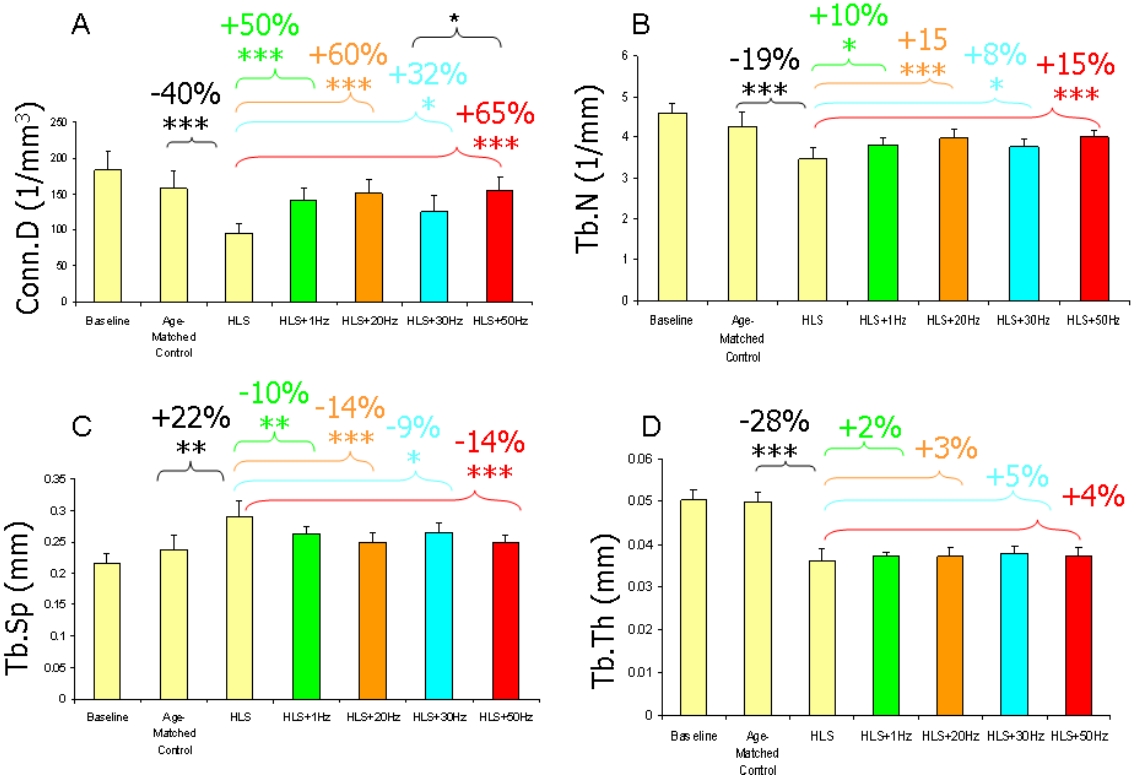

Figure 7. Bone morphology parameters changes upon disuse and application of dynamic muscle contractions. (A) Connectivity density, (B) Trabecular number, (C) Trabecular separation, (D) Trabecular thickness. (*p<0.05, **p<0.01, ***p<0.001)

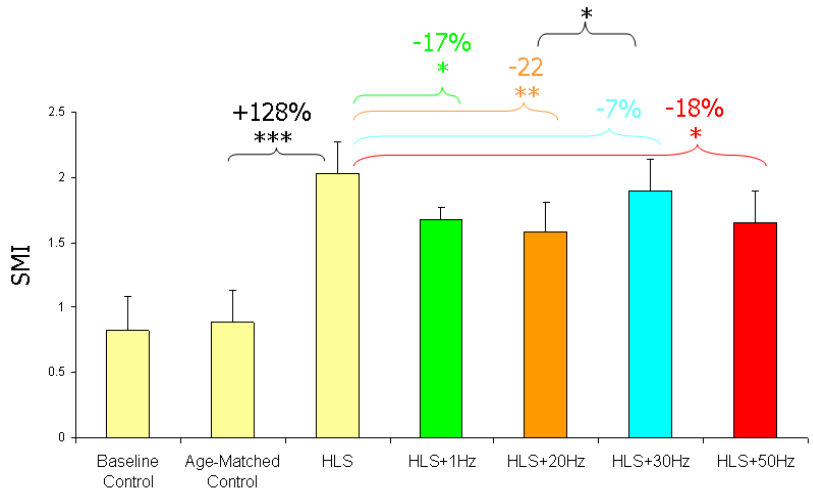

Figure 8. Structural model index (SMI) was significantly altered during disuse and showed increasing trends upon dynamic muscle stimulations. (*p<0.05, **p<0.01, ***p<0.001)

Cortical bone morphology also showed significant changes upon hind limb suspension, as indicated by a reduction of cortical area (-12%, p<0.01) (Figure 10). The periosteal envelope did not show significant changes (Figure 11C), while the endosteal enveloped decreased (-13%, p<0.05) (Figure 11D), indicating that most of the bone loss was induced by endosteal resorption. Maximum and minimum moments of inertia were also altered upon disuse (-13%, p<0.05; -9%) (Figure 11A, 11B). Intervention of the disuse with dynamic muscle stimulations increased cortical area at all frequencies including 1 Hz, (+6%, p<0.05), 20 Hz (+7%, p<0.05), 30 Hz (+8%, p<0.05), and 50 Hz (+10%, p<0.01) (Figure 10). Maximum and minimum moments of inertia were also enhanced by dynamic muscle contractions, with strongest attenuations observed at 50 Hz (+15%, p< 0.05) (Figure 11). Significant changes in periosteal and endosteal envelope were not detected upon muscle stimulation.

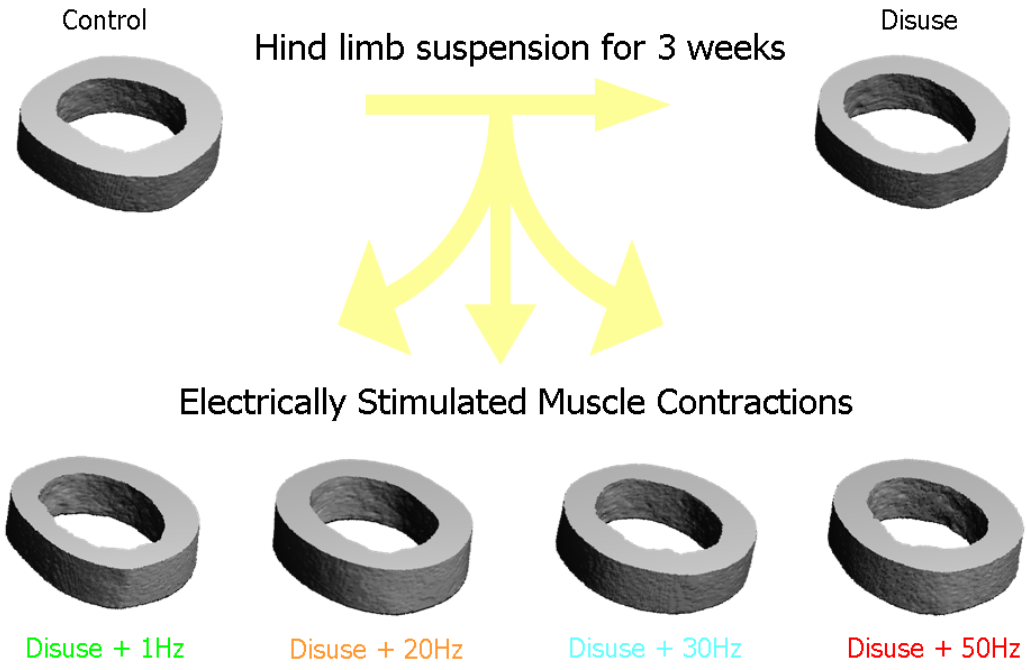

Figure 9. Three dimensional micro-computed tomographic images of cortical bone of the mid-diaphyseal femur upon hind limb suspension and dynamic muscle stimulations.

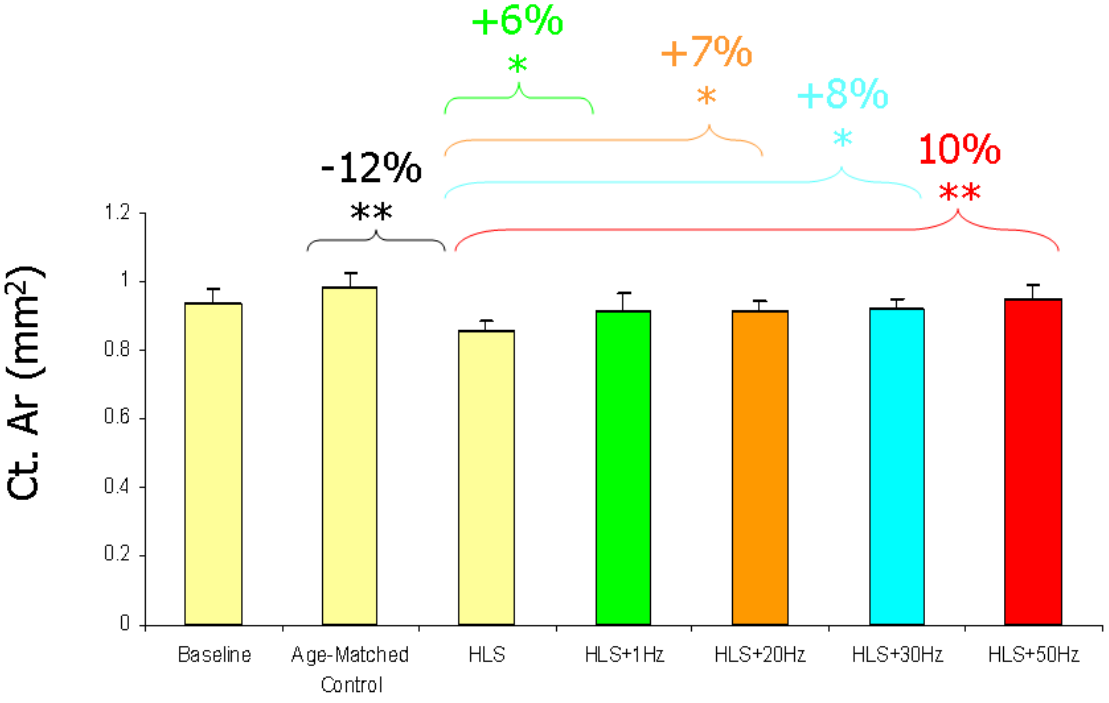

Figure 10. Cortical area showed significant changes upon disuse and the strongest attenuation was observed at 50 Hz muscle contractions. (*p<0.05, **p<0.01)

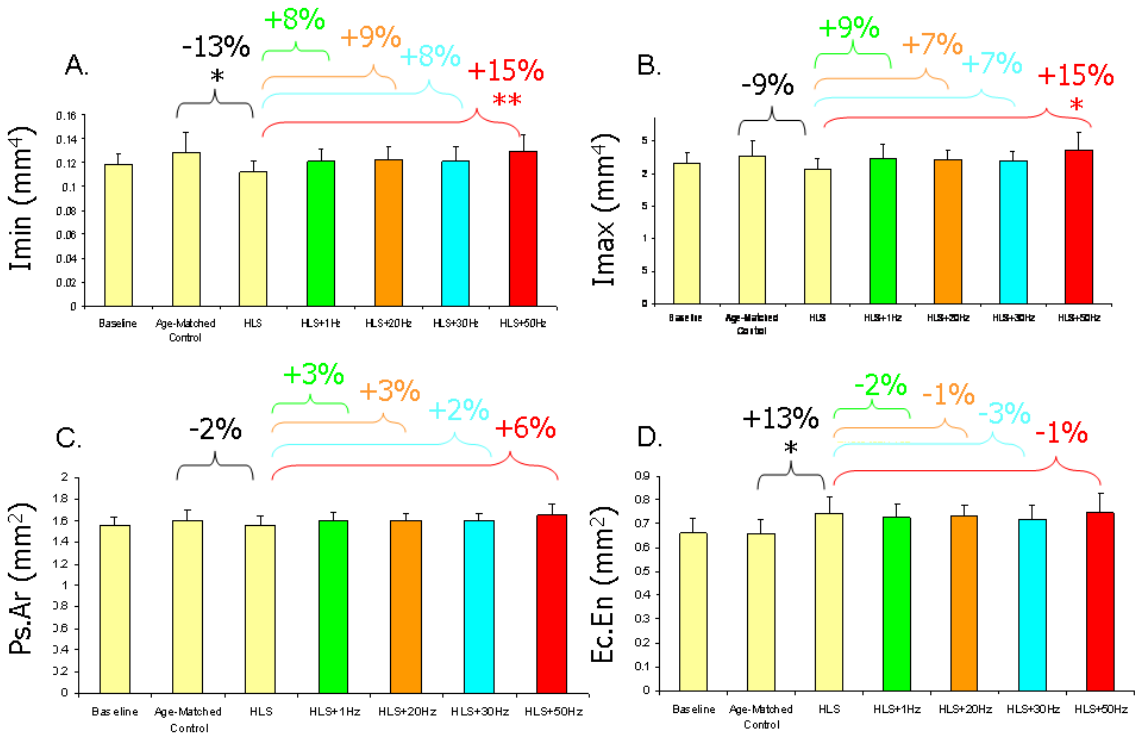

Figure 11. Cortical morphology alterations induced by disuse and application of dynamic muscle stimulations induced the strongest attenuation at 50 Hz. (A) Maximum moment of inertia, (B) Minimum moment of inertia, (C) Periosteal envelope, (D) Endocortical envelope. (*p<0.05)

Mechanical Testing

Analysis of a four-point bending test revealed significant reduction in stiffness (-21%, $p<0.01$) after 3 weeks of hind limb suspension (Table 4). Each stimulation group showed attenuation of bone tissue stiffness upon dynamic muscle stimulations at 1 Hz, (+6%), 20 Hz (+17%, $p<0.05$), 30 Hz (+15%), and 50 Hz (+13%), but only a significant increase was observed at 20 Hz (Table 4). The elastic modulus was significantly reduced by disuse when the last linear region was compared (-19%, $p<0.05$) (Table 5). Muscle stimulations also affected changes in elastic modulus at 20 Hz (+7%) and 30 Hz (+6%) (Table 5). The maximum force and stress experienced by the bone was significantly reduced with hind limb suspension (-24%, -17%, $p<0.05$) (Table 6). Muscle stimulations demonstrated attenuation of maximal force at 1 Hz, (+11%), 20 Hz (+23%), 30 Hz

(+11%), and 50 Hz (+28%, $p<0.05$) (Table 6). Stimulation at 50 Hz frequency demonstrated significant attenuation of the maximum force (Table 6).

Table 4. Changes in stiffness upon hind limb suspension and dynamic muscle stimulation. (asterisks indicate significant difference from hind limb suspension control: *p<0.05, **p<0.01, ***p<0.001)

		STIFFNESS (N/mm)			
		1st Region	**2nd Region**	**Last Region**	**All Regions**
Baseline Control	*mean ± SD*	180.1 ± 16.1	123.4 ± 9	123.4 ± 9	137.79 ± 21.5
Age-Matched Control	*mean ± SD*	190.9 ± 14.8	155.8 ± 21.6	142 ± 32.1	125 ± 8.9
HLS	*mean ± SD*	158.1 ± 10	108.8 ± 8	105.1 ± 13.8	99.2 ± 21.5
	% Loss	**- 21% ****	**- 30% *****	**- 28% ***	**- 21% ***
HLS + 1 Hz	*mean ± SD*	161.8 ± 17.4	124.9 ± 21.5	111.5 ± 30.6	103.8 ± 24.6
	% Attenuation	**+ 6%**	**+ 15%**	**+ 8%**	**+ 5%**
HLS + 20 Hz	*mean ± SD*	177.5 ± 18.5	127.2 ± 31.8	121.1 ± 39.4	116.2 ± 28.6
	% Attenuation	**+ 17% ***	**+ 17%**	**+ 18%**	**+ 18%**
HLS + 30 Hz	*mean ± SD*	174.3 ± 18	111.3 ± 14.4	112.3 ± 30.6	111 ± 17.5
	% Attenuation	**+ 15%**	**+ 2%**	**+ 9%**	**+ 13%**
HLS + 50 Hz	*mean ± SD*	171.7 ± 20.5	122.9 ± 59.5	127.4 ± 60.2	122.3 ± 31.3
	% Attenuation	**+ 13%**	**+ 13%**	**+ 24%**	**+ 24%**

Table 5. Changes in elastic modulus upon hind limb suspension and dynamic muscle stimulation. (asterisks indicate significant difference from hind limb suspension control: *p<0.05)

		Elastic Modulus (MPa)			
		1st Region	**2nd Region**	**Last Region**	**All Regions**
Baseline Control	*mean ± SD*	1783.7 ± 197.6	1189.4 ± 137.3	1189.4 ± 15.3	1378.1 ± 336
Age-Matched Control	*mean ± SD*	1699.3 ± 186.8	1393.1 ± 266.1	164.5 ± 15.7	1113.8 ± 118.2
HLS	*mean ± SD*	1592.1 ± 241.5	1134.8 ± 69	124.5 ± 10.4	1034.9 ± 267.5
	% Loss	**- 6%**	**- 18% ***	**- 19% ***	**- 7%**
HLS + 1 Hz	*mean ± SD*	1575.8 ± 211.4	1228.2 ± 195.9	1111.6 ± 363.7	1010.6 ± 247.6
	% Attenuation	**- 1%**	**+ 8%**	**+ 6.7%**	**- 2%**
HLS + 20 Hz	*mean ± SD*	1708.5 ± 193.1	1212.5 ± 255.7	1140.7 ± 284.2	1109.5 ± 223.4
	% Attenuation	**+ 7%**	**+ 7%**	**+ 9%**	**+ 7%**
HLS + 30 Hz	*mean ± SD*	1689 ± 208.5	1072.7 ± 99.3	1080.4 ± 275.8	1067.7 ± 123.9
	% Attenuation	**+ 6%**	**- 5%**	**+ 4%**	**+ 3%**
HLS + 50 Hz	*mean ± SD*	1561.2 ± 215.3	1097.4 ± 512.8	1129.9 ± 502.2	1104.4 ± 243.7
	% Attenuation	**- 2%**	**- 3%**	**+ 8%**	**+ 6.7%**

Table 6. Changes in the maximum force and stress, and the failure force and stress on the femur upon hind limb suspension and dynamic muscle stimulation. (asterisks indicate significant difference from hind limb suspension control: *p<0.05, **p<0.01)

		F_{max} (N)	σ_{max} (MPa)	$F_{failure}$ (N)	$\sigma_{failure}$ (MPa)
Baseline Control	*mean ± SD*	37.6 ± 4	73.7 ± 8.2	37.2 ± 4.2	72.9 ± 8.6
Age-Matched Control	*mean ± SD*	40.3 ± 3.9	76 ± 9.7	38 ± 4.9	70.6 ± 7.8
HLS	*mean ± SD*	30.5 ± 3	63.5 ± 7.3	26.3 ± 3	57.4 ± 6.1
	% Loss	**- 24% ****	**- 17% ***	**- 27% ****	**- 19% ****
HLS + 1 Hz	*mean ± SD*	33.9 ± 4.2	66.3 ± 8.8	31.4 ± 3.8	61.1 ± 5.8
	% Attenuation	**+ 11%**	**+ 4%**	**+ 13%**	**+ 6%**
HLS + 20 Hz	*mean ± SD*	37.4 ± 8.8	72 ± 13.6	35.6 ± 11.1	68.4 ± 18.5
	% Attenuation	**+ 23%**	**+ 13%**	**+ 29%**	**+ 19%**
HLS + 30 Hz	*mean ± SD*	33.7 ± 4.2	65.5 ± 8.8	31.2 ± 2.4	60.5 ± 3.8
	% Attenuation	**+ 11%**	**+ 3%**	**+ 13%**	**+ 5%**
HLS + 50 Hz	*mean ± SD*	39 ± 5.8	71.7 ± 10	33.9 ± 6.4	62.2 ± 11.1
	% Attenuation	**+ 28% ***	**+13%**	**+ 22.8%**	**+ 8%**

Muscle Wet Weight

The wet weight of the gastrocnemius, quadriceps, and whole limb was significantly reduced after hind limb suspension (-26%, $p<0.001$; -20%, $p<0.01$; -15%, $p<0.05$) (Table 7). Dynamic muscle stimulations showed significant attenuation in the whole limb wet weight at 20 Hz, 30 Hz and 50 Hz (+13%, +10.6%, +13%; $p<0.05$ for each) (Table 7).

Table 7. Alteration in the individual hind limb muscle wet weight and whole hind limb upon disuse and dynamic muscle contractions at frequencies from 1Hz to 50Hz. (asterisks indicate significant difference from hind limb suspension control: * $p<0.05$, ** $p<0.01$, ***$p<0.001$)

		Muscle Wet Weight (mg)			
		Soleus	**Gastrocnemius**	**Quadriceps**	**Whole Limb**
Baseline Control	*mean ± SD*	7.4 ± 2.3	138.3 ± 28.3	157.1 ± 79.7	807.4 ± 82.2
Age-Matched Control	*mean ± SD*	6.3 ± 1.5	122.6 ± 10.4	188.2 ± 21.2	751 ± 77
HLS	*mean ± SD*	4.7 ± 1.2	90.3 ± 12.8	150.8 ± 7.6	639.6 ± 55.8
	% Loss	**- 25%**	**- 26% *** **	**- 20% ** **	**- 15% ***
HLS + 1 Hz	*mean ± SD*	5.7 ± 2.2	96.7 ± 7.1	155.9 ± 9.3	683.8 ± 18.2
	% Attenuation	**+ 22%**	**+ 7.1%**	**+ 3.4%**	**+ 7%**
HLS + 20 Hz	*mean ± SD*	5 ± 1.1	98.8 ± 8.1	168.1 ± 11.2	722.1 ± 68.7
	% Attenuation	**+ 6%**	**+ 9.5%**	**+ 11.5%**	**+ 13% ***
HLS + 30 Hz	*mean ± SD*	4.9 ± 0.6	113.8 ± 20.4	149.4 ± 19	707.3 ± 44.7
	% Attenuation	**+ 3%**	**+ 26% ***	**- 1%**	**+ 10.6% ***
HLS + 50 Hz	*mean ± SD*	5 ± 0.5	106.2 ± 8	150.7 ± 18.2	722.2 ± 34.6
	% Attenuation	**+ 5%**	**+ 17.7%**	no change	**+ 13% ***

Muscle Morphology

Muscle fiber morphology analysis revealed a significant decrease in the average fiber cross sectional area (CSA) (-48%, $p<0.001$) (Table 8). Dynamic muscle contractions demonstrated attenuation of CSA from HLS control at 1 Hz, (+13%), 20 Hz (+38%), 30 Hz (+45%, $p<0.05$), and 50 Hz (+31%) (Table 8).

Table 8. Changes in average fiber cross sectional area (CSA) and fiber density upon hind limb suspension and dynamic muscle contraction. Significant attenuation of CSA was observed at 30 Hz. (Asterisks indicate significant difference from hind limb suspension control: * $p<0.05$, ** $p<0.01$, ***$p<0.001$)

		CSA (μm^2)	Fiber Density ($1/mm^2$)
Baseline Control	*mean ± SD*	2170.8 ± 333	302.8 ± 58.6
Age-Matched Control	*mean ± SD*	2764 ± 522.1	249.6 ± 61.8
HLS	*mean ± SD*	1410.7 ± 361.3	468.8 ± 115.3
	% Loss	**- 48% *** **	**+ 87.8% ** **
HLS + 1 Hz	*mean ± SD*	1595.8 ± 572.3	445.2 ± 150.2
	% Attenuation	**+ 13%**	**- 5%**
HLS + 20 Hz	*mean ± SD*	1955.1 ± 290.1	344.5 ± 73.5
	% Attenuation	**+ 38%**	**- 26.5%**
HLS + 30 Hz	*mean ± SD*	2039.1 ± 375.5	327.2 ± 109.3
	% Attenuation	**+ 45% ***	**- 30.2%**
HLS + 50 Hz	*mean ± SD*	1849.2 ± 419.1	380.7 ± 126.7
	% Attenuation	**+ 31%**	**- 18%**

DISCUSSION

The objective of this study was to evaluate the role of frequency (1 Hz – 50 Hz) on low magnitude, short duration, dynamic muscle contractions for preventing disuse induced bone loss and muscle atrophy. Stimulations at each frequency showed substantial attenuation of bone morphological, mechanical, and muscular morphological properties. The high frequency range from 20 Hz to 50 Hz demonstrated the strongest attenuation in both trabecular and cortical bone morphology. Two bone morphology parameters revealed differences between frequencies. 50 Hz stimulations showed significantly higher trabecular connectivity density when compared with 30 Hz. Also, the structural model index at 20 Hz was significantly different from SMI at 30 Hz. Mechanical testing revealed that the strongest attenuation in bone stiffness occurred with 20 Hz, while the 50 Hz showed strongest attenuation in the maximum force experienced by the bone. Muscle mass showed varying degrees of attenuation depending on the muscle group examined, however, the fiber cross sectional area showed strongest attenuation at 30 Hz. Overall, these results suggest that the musculoskeletal response varies with loading frequency, and strongest attenuation occurs in the 20 Hz to 50 Hz range. However, since significant differences were not detected between the stimulation frequencies for most of the parameters evaluated, an optimal frequency cannot be selected. Muscle stimulations did demonstrate potential to reduce the detrimental effects of disuse conditioning, and the varying response to frequency of stimulation may be explained by the difference in mechanical inputs, since each group received a different number of loading cycles during treatment. The musculoskeletal response seems to be enhanced with increasing loading cycles until about 20 Hz, thus, there may be a minimal

frequency required to obtain optimal responses. For example, extremely short exposure to dynamic loads have been shown to induce an anabolic response in bone (Rubin and Lanyon 1984), and thus, the number of loading cycles is critical to this musculoskeletal therapy. Our study suggests that the therapeutic potential may be enhanced at higher frequencies. Such an implication is consistent with studies that have shown that high frequency, low magnitude mechanical signals can prevent bone loss (Rubin, Xu et al. 2001), as higher frequency signals require lower orders of strain to induce an anabolic response (Qin, Rubin et al. 1998).

It has been hypothesized that muscle dynamics may alter bone intramedullary pressure (Winet 2003), a potential regulatory component of bone adaptation (Qin, Kaplan et al. 2003). Variations in loading parameters have been shown to influence musculoskeletal adaptation, and understanding their role is important for effective therapeutic designs (Martin, Burr et al. 1998). The results obtained in this study may potentially be explained by alterations in ImP; however, because the influence of fluid flow or other potential strain related parameters cannot be isolated in such a muscular therapeutic study, it is not clear whether the response observed is due solely to alterations in bone fluid flow. The role of frequency of dynamic muscle contractions has been controversial for muscular adaptation, whereas the relationship between frequency and bone adaptation to mechanical loading has been investigated. Increasing loading frequency significantly increases mechanically induced bone formation rates (Turner, Forwood et al. 1994). Other studies have demonstrated that only short durations of low magnitude, high frequency stimuli are required to induce an osteogenic response (Rubin, Xu et al. 2001). Although many studies have investigated chronic, low frequency

stimulations on muscular adaptation (Salmons and Henriksson 1981; Lieber 1986), a few studies have shown muscle response to short duration, high frequency stimulation (Mattiello-Sverzut, Carvalho et al. 2006; Kim, Roy et al. 2007). A short duration treatment regime for musculoskeletal disuse would be ideal, thus there is a need for optimization of such loading regimes. Therefore, the purpose of the first study in this thesis was to examine the frequency specificity of a loading period of 10 minutes per day via dynamic muscle contractions to prevent disuse induced bone loss.

Trabecular and cortical bone morphology demonstrated strongest attenuation at 20 Hz and 50 Hz dynamic muscle stimulations. However, the responses observed between these frequencies were not significantly different from each other. As demonstrated in several studies, although there may be a positive relation between loading frequency and bone adaptation, this may only exist up to a threshold level (Hsieh and Turner 2001; Warden and Turner 2004). It seems that with the loading parameters applied in this study, bone's adaptive response beyond 20 Hz does not induce any further attenuation of bone loss. As modulation of ImP has been suggested as a regulator of bone's osteogenic response, studies have examined the relationship between ImP and loading frequency. A murine knee loading model showed that the femoral ImP was significantly enhanced up to 10% above baseline ImP in the 20 Hz loading frequency range (Zhang, Su et al. 2006). ImP was not increased further at frequencies beyond 20 Hz. Although this threshold of ImP modulation may explain the similar response in bone morphology adaptation between 20 Hz and 50 Hz, this thesis only tested frequencies up to 50 Hz. An optimal threshold frequency of muscle stimulation cannot be determined based on this study

alone, since the response to muscle stimulation in the disuse mouse model beyond 50 Hz is not clear.

The mechanical strength testing performed in this study also showed significant attenuation at 20 Hz and 50 Hz. The stress-strain curves displayed several consecutive linear regions of successively decreasing slopes. Slopes of each individual region and all regions were compared, however, variability tended to increase. Multiple regions may have been observed because of movement of the bone sample during testing or microcracking. However, since the strain values are quite high within the first linear region, the first region will be considered most reliable with respect to stiffness and elastic modulus computations. The values obtained in this study for mouse femur stiffness and elastic modulus are comparable results of several other studies that have performed bending tests on the whole femur of skeletally mature mice. In this study, we obtained stiffness values ranging from 150 N/mm to 200 N/mm. The bone tissue stiffness can vary among skeletally mature mice of varying strain from 50 N/mm to 500 N/mm (Simske, Greenberg et al. 1991; Turner and Burr 1993; Jamsa, Jalovaara et al. 1998; Akhter, Cullen et al. 2001; Hanson, Ferguson et al. 2005; Bensamoun, Hawse et al. 2006; Wallace, Rajachar et al. 2007). Thus, the range of values obtained in this study for elastic modulus (between 1 GPa to 2 GPa) have also been demonstrated in whole femur bending tests of adult mice (Jamsa, Jalovaara et al. 1998). Similarly, the ultimate deformation and strain values of this study are comparable with results obtained from similar mechanical testing experiments with adult mouse hind limb bones of similar geometry (Bensamoun, Hawse et al. 2006). Comparing the tissue stiffness at the first region showed significant attenuation from hind limb suspension at 20 Hz dynamic muscle contractions, while

comparison of the maximum force experienced resulted in a significant difference at 50 Hz stimulation. Maximum and minimum moment of inertia also demonstrated greatest attenuation at 50 Hz stimulations. Thus, stimulation at the 20 Hz to 50 Hz range may increase resistance to fracture. These results seem consistent with the responses observed with bone morphology adaptation, suggesting that modulation of ImP via dynamic muscle contractions may be regulating bone's morphological and mechanical response.

Bone's response seems to be enhanced with increasing loading frequency. However, the trabecular bone morphology data presented in this study does not seem to agree with this trend for 30 Hz stimulations. Whereas 20 Hz and 50 Hz demonstrate substantial attenuation of bone volume fraction, connectivity density, and trabecular number, 30 Hz stimulations show a diminished response. Connectivity density at 30 Hz was actually significantly lower than with 50 Hz stimulations. Although such a response was not as apparent in cortical morphology upon 30 Hz stimulations, mechanical testing data did suggest a similar trend in which 30 Hz stimulations resulted in a weaker response when compared with 20 Hz and 50 Hz. However, difference between stimulation frequencies were not detected, therefore, the results of an apparent differential response at 30 Hz are not conclusive and should be repeated to confirm if this frequency does generate a diminished response.

Muscular adaptation to dynamic muscle contractions demonstrated that 30 Hz frequency has the strongest potential to reduce disuse induced muscle atrophy. Muscle mass and fiber cross sectional area (CSA) are indicative of muscular strength, since fibers of larger diameters can generate greater tension (Lieber 1986). Gastrocnemius muscle wet weight was significantly greater than hind limb suspension at 30 Hz stimulations, and

similarly, the mean fiber CSA showed significant differences from disuse at 30 Hz. Although only the electrical stimulation was applied to the quadriceps muscles, these data show that other hind limb muscles of the posterior compartment were substantially affected. During each 2 second bout of muscle stimulation, a full plantar flexion is consistently observed, thus it is likely that the gastrocnemius, soleus, and plantaris muscles are influenced by the stretch magnitude experienced, and need not experience contraction to induce an adaptive response. Other studies have demonstrated similar effects in which the tibialis anterior muscle was stimulated directly, however, a strong response was observed on the unstimulated soleus muscle (Lieber, Ferro et al. 1988). Stretch has been demonstrated as an important mechanical signal with potential to stimulate muscle protein synthesis and muscle growth (Goldspink 1964; Loughna, Goldspink et al. 1986). Muscle stretch in the immobilized limb can influence gene expression in muscle (Loughna, Izumo et al. 1990) and thus protein expression, regulating muscular phenotype and its adaptive response.

Studies have suggested a wide range of therapeutic frequencies for muscular adaptation; however the results are highly dependent on other loading parameters such duration of treatment and insertion of recovery periods. Electrical stimulation can synchronously activate fibers whereas voluntary contractions recruit fibers preferentially. Thus electrical stimulation is effective in inducing an immediate adaptive response. The morphological alterations observed upon electrical stimulation include fiber type transformation, increased capillary density and increased resistance to fatigue. Many studies have examined the role of long term, low frequency stimulation for preventing muscle atrophy, particularly for slow twitch fibers (Dupont Salter, Richmond et al. 2003).

However, other studies have demonstrated that high frequency stimulations are required to activate the fast twitch fibers, and short duration treatments have been shown to recover fiber CSA and muscle mechanical properties after immobilization (Mattiello-Sverzut, Carvalho et al. 2006). The results of this study do demonstrate attenuation in the high frequency range when stimulations are applied for short durations (10 minutes per day). However, to improve the muscular response, studies have indicated that insertion of rest periods is essential during high frequency treatments to prevent onset of muscle fatigue.

This study attempts to evaluate electrical stimulation as a combined treatment for muscle and bone, and to optimize loading parameters required to induce musculoskeletal adaptation. The results seem to suggest a differential optimal response between bone and muscle. The musculoskeletal adaptive response relies on the proposed mechanisms each individual system. Whereas modulation of bone ImP is hypothesized as a key regulatory component of bone adaptation via muscle dynamics, muscular adaptation to electrical stimulations seems to rely on increased demand, preferential activation of muscle fibers, and minimized fatigue. High frequency electrical stimulations result in muscle contractions near the tetanic range where individual muscle twitch responses cannot be distinguished, and the tension generated by muscle fibers reach maximal levels. In human muscle, tetanic responses begin to be observed at stimulation frequencies above 30 Hz (Widmaier, Raff et al. 2004). However, in the mouse model, tetanic responses may not be induced until stimulation frequencies reach 300 Hz (Lieber 1986; Lieber 1988). It may not be necessary to use tetanic contractions to induce a healthy muscular response, but literature suggests that high frequency stimulation may enhance muscle adaptation via

increased force generation. If true, such high frequency loading may be extended to enhance osteogenesis, since bone's response has been shown to increase with higher frequencies. This study does demonstrate the ability of muscle dynamics to induce a positive adaptive response in both bone and muscle in the high frequency range of 20 Hz to 50 Hz, thus affirming such a loading regime for treatment of musculoskeletal disuse.

CHAPTER 4: ROLE OF RECOVERY PERIODS ON DYNAMIC MUSCLE CONTRACTIONS

ABSTRACT

Dynamic muscle contractions have been proposed to induce musculoskeletal adaptation via modulation of bone intramedullary pressure. Preliminary studies have demonstrated that dynamic muscle contractions within an optimal frequency range can significantly attenuate disuse induced bone loss. However, the optimal rest periods required to prevent muscle fatigue during stimulations are not clear. The overall objective of this study was to evaluate optimized dynamic muscle stimulations at 20 Hz, and to evaluate the insertion of a five minute rest-insertion on musculoskeletal adaptation in a functional hind limb disuse mouse model. Thirty-five adult female BALB/c mice were randomized into 5 groups: baseline control (n=6), age-matched control (n=6), hind limb suspension non-stimulated (HLS-NS) (n=8), and HLS with electrically stimulated muscle contractions at 20 Hz for a continuous 10 minutes (n=8) or with a 5 minute recovery period inserted between two 5-minute loading bouts (n=7). Pulsatile signal was delivered to the quadriceps muscles for 2 seconds, followed by 3 second rest period, for total of 10 minutes per day, for 3 weeks. Comparison with HLS control showed that both trabecular and cortical bone morphology parameters were substantially increased in both continuous and rest-inserted groups, including trabecular bone volume fraction (+47%, $p<0.01$; +35%), and cortical area (+7%, $p<0.05$; +10%, $p<0.01$). However, only rest-inserted signals showed significant attenuation in bone mechanical strength parameters such as maximum force (+42%, $p<0.01$) and muscle fiber CSA (+44%, $p<0.05$). These data suggest the rest-insertions during dynamic muscle stimulations at 20 Hz have potential to enhance musculoskeletal adaptation, possibly via modulation of intracortical

fluid flow. Further studies of optimization may elucidate the optimal signal parameters required for designing a preventive treatment for musculoskeletal disuse.

INTRODUCTION

Musculoskeletal disuse causes severe physiologic changes and it has been proposed that synergistic effects of muscle function and bone adaptation may play a role in developing a countermeasure. The skeletal muscle pump may be involved in bone adaptation and bone mechanotransduction via modulation of intracortical fluid pressure gradients. Thus, muscular stimulation may be used to simultaneously treat muscle and bone, but the optimal parameters required for such treatment is unclear. Studies have separately investigated the optimal signal parameters for bone or muscle. Insertion of recovery periods during high frequency stimulations have shown potential to reduce muscle atrophy by minimizing fatigue and mimicking physiologic contractions (Prentice 2002). The benefit of recovery periods have also been demonstrated in bone, and the underlying mechanism of the enhanced bone adaptation is related to the concept of the saturation curve of mechanosensitivity. Osteocytes, the most abundant cells found in bone tissue, can respond to fluid flow (Klein-Nulend, Semeins et al. 1995). It has been shown that mechanical loading increases fluid flow and diffusion inside bone (Knothe Tate, Steck et al. 2000). However, since the fluid within the canalicular network has been shown to be highly viscous (Zhu, Lai et al. 1991), there may exist an inertial damping effect. Previous studies have demonstrated that short bouts of high frequency stimulation may enhance musculoskeletal adaptation (Robling, Burr et al. 2001; Robling, Hinant et al. 2002; Srinivasan, Weimer et al. 2002; LaMothe and Zernicke 2004). Insertion of short or long term recovery periods have been suggested to enhance osteogenesis, potentially re-sensitizing bone cells and diminishing inertial fluid flow effects. There are very few studies that have examined the role of such parameter on the

combined response of muscle and bone. Therefore, there is a need to investigate the effects of various types of rest insertions in muscle stimulations to simultaneously benefit muscle and bone. Recovery periods on the order of 10 seconds (Srinivasan, Weimer et al. 2002), and separating short loading bouts with 3 hours of rest (Robling, Hinant et al. 2002) have been shown enhance osteogenesis. With respect to muscle adaptation, a recent study has revealed significant attenuation in muscle strength and phenotype when high frequency muscle stimulations of 5 minute duration were separated by 5 minute recovery periods (Kim, Roy et al. 2007). Bone cells have been shown to respond to the first few minutes of loading (Rubin and Lanyon 1984), and in vitro studies have shown that maximal response to fluid flow are observed in the first 5 minutes of stimulation (Klein-Nulend, Semeins et al. 1995). Thus, although recovery periods beneficial to bone have been defined on several scales (from seconds to hours), a recovery period of 5 minutes inserted between two 5 minute loading bouts will be investigated in this study, since there is evidence of bone adaptation to extremely short periods of loading and recent studies demonstrate muscle enhancement with 5 minute rests . Preliminary studies discussed in Chapter 3 indicate significant bone adaptation when subjected to muscle stimulation at 20 Hz with a two second on to 3 second off repeated rest ratio, thus the same signal will be used to evaluate the role of a 5 minute recovery period. Therefore, the hypothesis of this study was that insertion of a 5 minute recovery period between two 5 minutes bouts of muscle stimulation at 20 Hz will enhance trabecular and cortical morphology, bone mechanical strength, and muscle fiber morphology.

MATERIALS AND METHODS

Animal Model

Thirty-five adult female BALB/cByJ mice were randomized into 5 groups: baseline control, age-matched control, hind limb suspension non-stimulated (HLS-NS), HLS with a continuous 20 Hz muscle stimulation, or with a rest inserted 20 Hz muscle stimulation (Table 9). The hind limb suspension model was used in this study is described in detail in Chapter 3.

Table 9. Experimental design.

Group	N
Baseline Control	6
Age-Matched Control	6
HLS	8
HLS + Continuous 20Hz	8
HLS + Rest-Inserted 20 Hz	7

Signal and Stimulation

Dynamic muscle stimulations were applied to the right quadriceps muscles of each hind limb suspended mouse. The signal parameters used in this study are consistent with the protocol described in Chapter 3. Two stimulation regimes were compared: a continuous and a rest-inserted 20 Hz stimulation. The continuous signal is the same signal applied in the previous study described in Chapter 3, however, the rest-inserted signal was applied for 5 minutes, followed by a 5 minute recovery period, followed by another 5 minutes of stimulation (Figure 12).

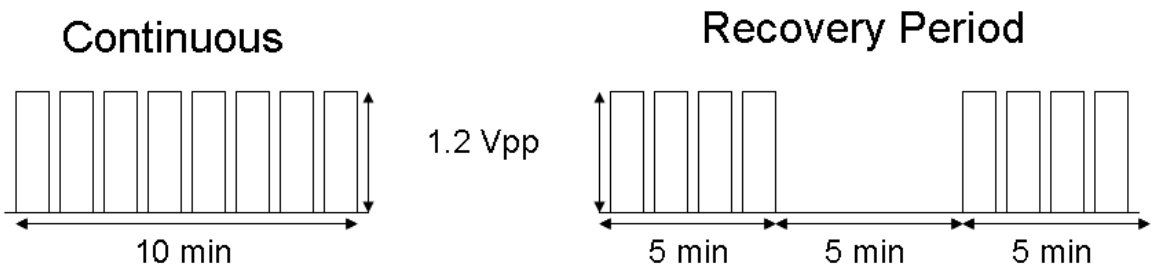

Figure 12. Schematic of signals applied to the right quadriceps muscles during hind limb suspension.

Analysis of Bone Morphology, Bone Strength, and Muscle Morphology

At the end of the 3 week experiment animals were sacrificed and hind limb muscles were dissected and weighed, and quadriceps muscles were prepared for histological analysis. The right femurs were scanned using Micro-CT for trabecular and cortical morphology analysis. Bone samples were subsequently prepared for mechanical testing and underwent a four-point bending test. Muscle histological analysis was done to quantify changes in fiber CSA and fiber density. Detailed procedures of each of these analyses are described in the Methods and Materials section of Chapter 3.

Statistics

As described in Chapter 3, all data were analyzed using ANOVA and significance between groups was determined using Tukey's method of post-hoc comparisons, at a significance level of 0.05.

RESULTS

Bone Morphology

Trabecular bone morphology analysis demonstrated attenuation from HLS control with both continuous (+46%, $p<0.05$) and rest-inserted signal (+35, $p>0.05$) (Figure 14). Rest-inserted attenuation was not significantly different from hind limb suspension control, or from the continuous signal. Significant attenuation of trabecular connectivity density (+60%, $p<0.01$; +43%, $p<0.05$) and trabecular number (+15%, $p<0.01$; +12%, $p<0.01$) were observed in both continuous and rest-inserted signals, however, the continuous signal showed a higher significance from hind limb suspension control (Figure 15). Trabecular separation decreased significantly with both stimulations (-14%, $p<0.01$; -11%, $p<0.05$), but a higher significance was observed with the continuous signal (Table 10). However, the structural model index was significantly altered only with the continuous signal (-22%, $p<0.05$) (Table 9).

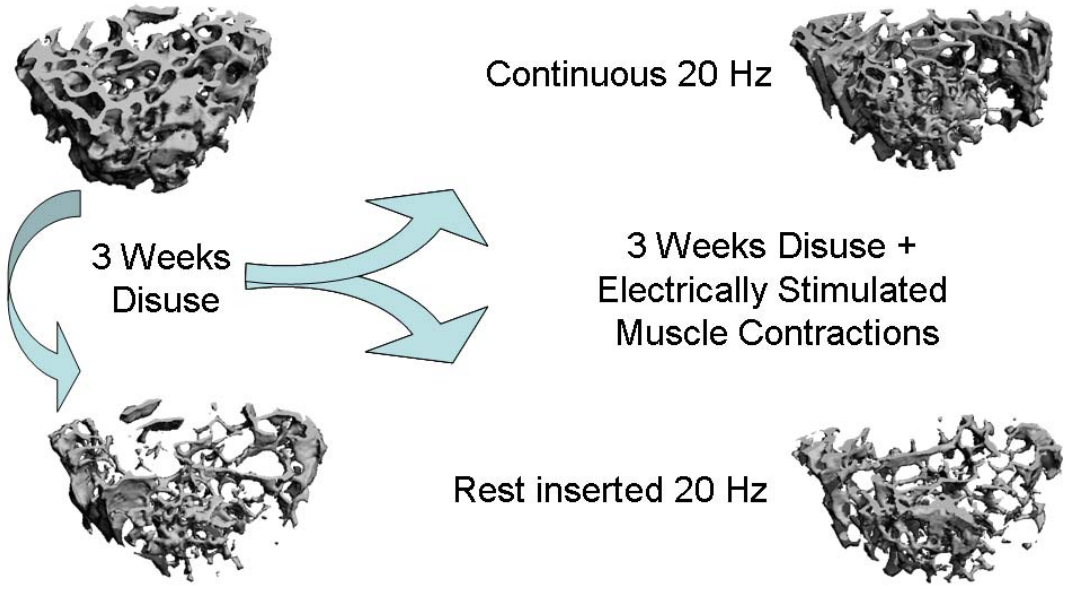

Figure 13. Three dimensional micro-computed tomographic images of metaphyseal trabecular bone of the distal femur upon disue and dynamic muscle stimulations with and without a recovery period.

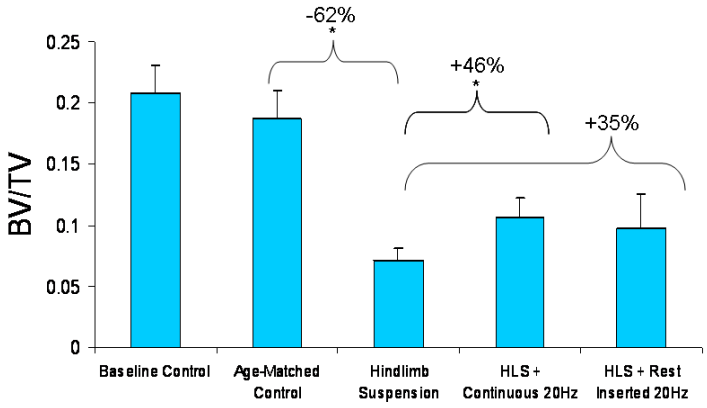

Figure 14. Bone volume fraction was reduced upon HLS, and dynamic muscle contractions demonstrated significant attenuation at only with the continuous 20 Hz signal. (*p<0.05)

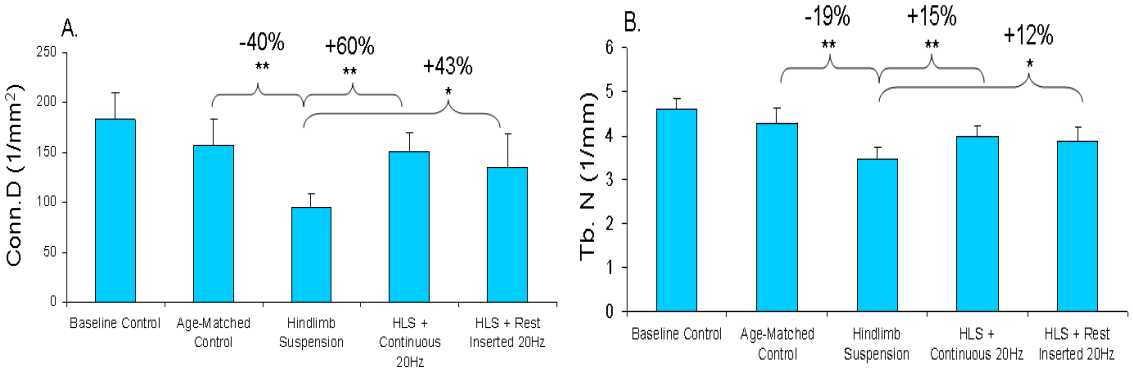

Figure 15. Bone morphology parameters changes upon disuse and application of dynamic muscle contractions. (A) Connectivity density, (B) Trabecular number. (*<0.05, **p<0.01)

Table 10. Alterations in trabecular thickness, trabecular separation, and structural model index upon disuse and application of continuous and rest-inserted dynamic muscle contractions. (*p<0.05, **p<0.01)

		Tb.Th (mm)	Tb.Sp (mm)	SMI
Baseline Control	*mean ± SD*	0.0504 ± 0.002	0.2167 ± 0.014	0.8226 ± 0.259
Age-Matched Control	*mean ± SD*	0.0497 ± 0.002	0.2378 ± 0.022	0.8892 ± 0.243
HLS	*mean ± SD*	0.036 ± 0.003	0.0291 ± 0.024	2.033 ± 0.241
	% Loss	**- 28% ****	**+ 22% ***	**+ 128% ****
HLS + 20 Hz Continuous	*mean ± SD*	0.0371 ± 0.002	0.2496 ± 0.015	1.58 ± 0.232
	% Attenuation	**+ 3%**	**- 14% ****	**- 22% ***
HLS + 20 Hz Rest-Inserted	*mean ± SD*	0.0379 ± 0.002	0.258 ± 0.02	1.8381 ± 0.428
	% Attenuation	**+ 5%**	**- 11% ***	**- 10%**

Cortical bone morphology demonstrated trends opposite from the trabecular morphology results. Cortical area (+6%, $p<0.05$; +10%, $p<0.01$) and cortical thickness (+4%, $p<0.05$; +7%, $p<0.01$) demonstrated attenuation with both the continuous and rest-inserted signal (Figure 17A, 17B), however, higher significance was generally observed with the rest-inserted stimulation. Differences between the two stimulation regimes were not detected. No changes were detected in periosteal envelope, however, endocortical envelope increased from HLS control with rest-inserted stimulation (-8%) (Figure 17C, 17D). Maximum (+7%, +9%) and minimum moment of inertia (+9%) showed attenuation but these changes were not significantly different from hind limb suspension control (Table 11).

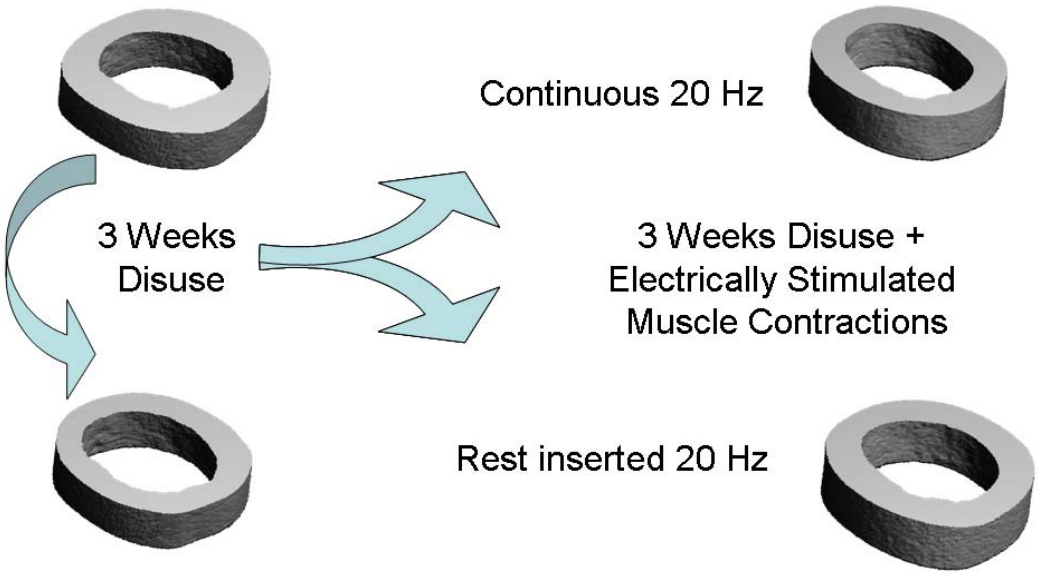

Figure 16. Three dimensional micro-computed tomographic images of cortical bone of the mid-diaphyseal femur upon disuse and dynamic muscle stimulations.

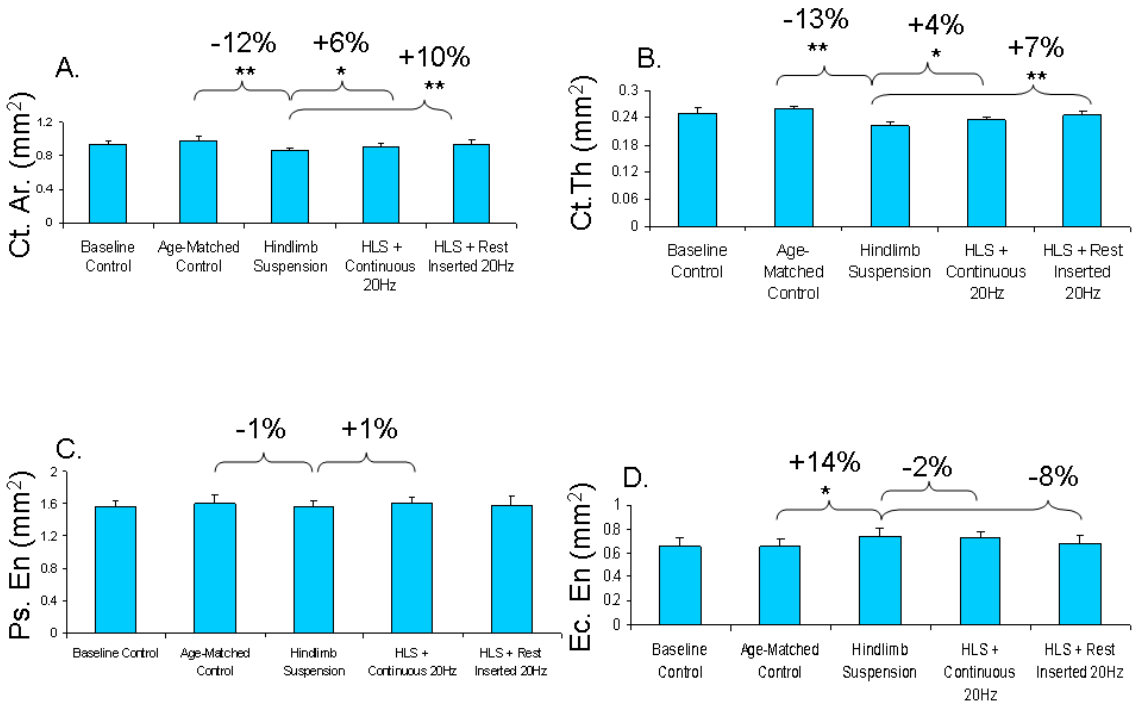

Figure 17. Cortical area (A) and cortical thickness (B) showed significant attenuation with both continuous and rest-inserted signals. Periosteal envelope (C) was not affected, and endocortical envelope (D) showed attenuation but changes were not significant (*p<0.05, **p<0.01)

Table 11. Alterations in maximum moment of inertia (A), and minimum moment of inertia (B) induced by disuse and application of dynamic muscle stimulations (*p<0.05)

		I_{max} (mm^4)	I_{min} (mm^4)
Baseline Control	*mean ± SD*	0.217 ± 0.0168	0.1182 ± 0.009
Age-Matched Control	*mean ± SD*	0.2262 ± 0.025	0.1286 ± 0.016
HLS	*mean ± SD*	0.206 ± 0.017	0.112 ± 0.009
	% Loss	**- 9% ***	**+ 13% ***
HLS + 20 Hz Continuous	*mean ± SD*	0.2216 ± 0.014	0.1219 ± 0.012
	% Attenuation	**+ 7%**	**+ 9%**
HLS + 20 Hz Rest-Inserted	*mean ± SD*	0.2159 ± 0.027	0.1225 ± 0.016
	% Attenuation	**+ 5%**	**+ 9%**

Mechanical Testing

Four-point bending analysis allowed comparison of mechanical strength parameters between the continuous and rest-inserted loading regimes. Both stimulations showed attenuation, however, only the rest-inserted group showed significant attenuation. Tissue stiffness was enhanced from HLS control at the continuous and rest-inserted group (+17%; +23%, $p<0.05$) (Table 12). The stiffness observed in the 2nd region was significantly different between the rest inserted and continuous group ($p<0.05$). Similarly, the elastic modulus was significantly enhanced with the rest-inserted group only, at the 2nd (+34%, $p<0.01$) and last linear regions (+40%, $p<0.01$) of the stress strain curve (Table 13). For both of these regions, the elastic modulus between the rest-inserted group and the continuous group were significantly different from each other ($p<0.05$) (Table 13). In addition, the maximum force (+23%; +42%, $p<0.01$) and stress (+13%, +33%, $p<0.01$), and failure force (+29%; +43%, $p<0.05$) and stress (+19%; +35%, $p<0.05$) experienced by the continuous and rest-inserted stimulations were greater than hind limb suspension control; only the rest-inserted signal induced significant changes (Table 14).

Table 12. Changes in stiffness upon hind limb suspension and dynamic muscle stimulation. (asterisks indicate significant difference from hind limb suspension control: *p<0.05, **p<0.01, ***p<0.001; # indicates significant differences between continous and rest-inserted signals: #p<0.05)

		STIFFNESS (N/mm)			
		1st Region	**2nd Region**	**Last Region**	**All Regions**
Baseline Control	*mean ± SD*	180.1 ± 16.1	123.4 ± 9	123.4 ± 9	137.79 ± 21.5
Age-Matched Control	*mean ± SD*	190.9 ± 14.8	155.8 ± 21.6	142 ± 32.1	125 ± 8.9
HLS	*mean ± SD*	158.1 ± 10	108.8 ± 8	105.1 ± 13.8	99.2 ± 21.5
	% Loss	**- 21% ****	**- 30% *****	**- 28% ***	**- 21% ***
HLS + 20 Hz Continuous	*mean ± SD*	177.5 ± 18.5	127.2 ± 31.8	121.1 ± 39.4	116.2 ± 28.6
	% Attenuation	**+ 17%**	**+ 17%**	**+ 18%**	**+ 18%**
HLS + 20 Hz Rest-Inserted	*mean ± SD*	186.8 ± 24.6	159.9 ± 18.4	154.2 ± 28.8	133.8 ± 27
	% Attenuation	**+ 23% ***	**+ 47% ** #**	**+ 50% ***	**+ 36%**

Table 13. Changes in elastic modulus upon hind limb suspension and dynamic muscle stimulation. (asterisks indicate significant difference from hind limb suspension control: *p<0.05 **p<0.01; # indicates significant differences between continous and rest-inserted signals: #p<0.05)

		ELASTIC MODULUS (MPa)			
		1st Region	**2nd Region**	**Last Region**	**All Regions**
Baseline Control	*mean ± SD*	1783.7 ± 197.6	1189.4 ± 137.3	1189.4 ± 15.3	1378.1 ± 336
Age-Matched Control	*mean ± SD*	1699.3 ± 186.8	1393.1 ± 266.1	164.5 ± 15.7	1113.8 ± 118.2
HLS	*mean ± SD*	1592.1 ± 241.5	1134.8 ± 69	124.5 ± 10.4	1034.9 ± 267.5
	% Loss	**- 6%**	**- 18% ***	**- 19% ***	**- 7%**
HLS + 20 Hz Continuous	*mean ± SD*	1708.5 ± 193.1	1212.5 ± 255.7	1140.7 ± 284.2	1109.5 ± 223.4
	% Attenuation	**+ 7%**	**+ 7%**	**+ 9%**	**+ 7%**
HLS + 20 Hz Rest-Inserted	*mean ± SD*	1795.5 ± 258.6	1531.8 ± 139.4	1463.2 ± 169	1272.7 ± 188.5
	% Attenuation	**+ 23%**	**+ 34% ** #**	**+ 40% ** #**	**+ 36%**

Table 14. Alterations in the maximum force and stress, and the failure force and stress on the femur upon hind limb suspension and dynamic muscle stimulation with rest-inserted and continuous stimulations. (asterisks indicate significant difference from hind limb suspension control: *p<0.05, **p<0.01)

		F_{max} (N)	σ_{max} (MPa)	$F_{failure}$	$\sigma_{failure}$
Baseline Control	*mean ± SD*	37.6 ± 4	73.7 ± 8.2	37.2 ± 4.2	72.9 ± 8.6
Age-Matched Control	*mean ± SD*	40.3 ± 3.9	76 ± 9.7	38 ± 4.9	70.6 ± 7.8
HLS	*mean ± SD*	30.5 ± 3	63.5 ± 7.3	26.3 ± 3	57.4 ± 6.1
	% Loss	**- 24% ** **	**- 16.5% ***	**- 27% ** **	**- 19% ** **
HLS + 20 Hz Continuous	*mean ± SD*	37.4 ± 8.8	72 ± 13.6	35.6 ± 11.1	68.4 ± 18.5
	% Attenuation	**+ 23%**	**+ 13%**	**+ 29%**	**+ 19%**
HLS + 20 Hz Rest-Inserted	*mean ± SD*	43.3 ± 4.1	84.5 ± 7.2	39.4 ± 5.3	77.3 ± 12.6
	% Attenuation	**+ 42% ** **	**+ 33% ** **	**+ 43% ***	**+ 35% ***

Muscle Wet Weight

The wet weight of individual hind limb muscles showed that soleus muscle was similar between the two stimulation groups, but were not significantly higher than hind limb suspension control. The weight of the gastrocnemius muscle was enhanced

compared with disuse control (+10%; +20%, $p<0.05$), but quadriceps showed significant changes with continuous stimulation (+12%, $p<0.01$) (Table 15).

Table 15. Adaptations in the individual hind limb muscle wet weight and whole hind limb upon disuse and dynamic muscle contractions at continuous and rest-inserted stimulations. (asterisks indicate significant difference from hind limb suspension control: * $p<0.05$, ** $p<0.01$, ***$p<0.001$; # indicates significant differences between continuous and rest-inserted stimulations).

		Muscle Wet Weight (mg)			
		Soleus	**Gastrocnemius**	**Quadriceps**	**Whole Limb**
Baseline Control	*mean ± SD*	7.4 ± 2.3	138.3 ± 28.3	157.1 ± 79.7	807.4 ± 82.2
Age-Matched Control	*mean ± SD*	6.3 ± 1.5	122.6 ± 10.4	188.2 ± 21.2	751 ± 77
HLS	*mean ± SD*	4.7 ± 1.2	90.3 ± 12.8	150.8 ± 7.6	639.6 ± 55.8
	% Loss	**- 25%**	**- 26% *** **	**- 20% ** **	**- 15% ***
HLS + 20 Hz Continuous	*mean ± SD*	5 ± 1.1	98.8 ± 8.1	168.1 ± 11.2	722.1 ± 68.7
	% Attenuation	**+ 6%**	**+ 10%**	**+ 12% ** **	**+ 13%**
HLS + 20 Hz Rest-Inserted	*mean ± SD*	5 ± 1.9	108.5 ± 11.5	146.4 ± 7.8	702 ± 67.1
	% Attenuation	**+ 6.3%**	**+ 20% ***	**- 3% #**	**+ 9.8%**

Muscle Morphology

Analysis of muscle histology demonstrated a strong response with the rest inserted stimulation (+44%, $p<0.05$) . The continuous stimulation also showed increasing trends, but this change was not significant. Fiber density showed increasing trends with continuous (-27%) and rest inserted (-26%) signals but these changes were not significant (Table 16).

Table 16. Changes in average fiber cross sectional area (CSA) and fiber density upon hind limb suspension and dynamic muscle contraction. Significant attenuation of CSA was observed at with rest-inserted stimulations. (* p<0.05, ** p<0.01, ***p<0.001)

		CSA (μm^2)	Fiber Density ($1/mm^2$)
Baseline Control	*mean ± SD*	2170.8 ± 333	302.8 ± 58.6
Age-Matched Control	*mean ± SD*	2764 ± 522.1	249.6 ± 61.8
HLS	*mean ± SD*	1410.7 ± 361.3	468.8 ± 115.3
	% Loss	**- 48% *** **	**+ 87.8% ** **
HLS + 20 Hz Continuous	*mean ± SD*	1955.1 ± 290.1	344.5 ± 73.5
	% Attenuation	**+ 38%**	**- 27%**
HLS + 20 Hz Rest-Inserted	*mean ± SD*	2035.9 ± 668	345.1 ± 106
	% Attenuation	**+ 44% ***	**- 26%**

DISCUSSION

This objective of this study was to evaluate the role of a short recovery period in a low magnitude, high frequency, dynamic muscle stimulation as a preventive treatment for musculoskeletal system. A 20 Hz stimulation frequency was selected to evaluate the role of recovery periods because previous studies demonstrated significant potential to induce musculoskeletal adaptation. Trabecular and cortical bone morphology data demonstrated that significant attenuation can be achieved with both a continuous and rest-inserted signal. However, trabecular data tends to show stronger attenuation with continuous stimulation, while cortical data tends to show higher significance with rest-inserted stimulation. The bone morphological data alone does not allow us to draw conclusions about the influence of the rest-insertion because significant differences between the two stimulation regimes were not detected.

On the other hand, mechanical testing data and muscle morphology data did demonstrate a differential response between the continuous and rest-inserted stimulations. Bone tissue stiffness was significantly higher than hind limb suspension control at all linear regions analyzed. Stiffness of the rest-inserted group in the second region was found to be significantly different from the continuous group. Elastic modulus also showed significant attenuation only with rest-inserted groups, and these changes were also significantly different from continuous groups. Finally, comparison of the maximum and failure force and stresses experienced by the bone indicated that rest-inserted stimulations induced significant attenuation from disuse. While continuous stimulations did show increasing trends, the changes were not statistically significant. Although the number of loads applied during the continuous and rest-inserted signal was equal, the

difference in response may be due to recovery of mechanosensitivity of bone cells. While trabecular bone may show strongest response in high frequency stimulation without any rest-insertions, cortical morphology suggests slightly higher increasing with rest-insertions. The improvement in cortical morphology may explain the stronger mechanical response, thus rest-insertions may enhance bone's resistance to fracture. In addition, analysis of muscle morphology demonstrated that rest-inserted stimulations can induce significant changes in fiber CSA. This response may be attributed to minimized muscle fatigue experienced during the recovery period.

The role of recovery periods during mechanical stimulation has been investigated in this study in order to attempt to optimize both the skeletal and muscular adaptive response. Because there is a differential mechanism of response of these two systems, the rationale for recovery periods is particular to the tissue type. Muscle stimulations preferentially recruit fast fibers before slow twitch fibers, and because low resistance to fatigue is property of the faster fibers, there is a need for recovery periods. Rests insertions can help to minimize fatigue, but are also applied because they mimic the dynamic nature of physiologic contractions.

The type of fiber also determines the type of contraction required for activation. While slow fibers are activated during chronic, low frequency stimulations, fast fibers require short duration, high frequency stimulations for intermittent activation. Several studies have demonstrated the ability of high frequency muscle stimulation to reduce muscular atrophy (Delitto and Snyder-Mackler 1990; Sinacore, Delitto et al. 1990; Qin, Appell et al. 1997; Mattiello-Sverzut, Carvalho et al. 2006). A recent study showed that brief periods of muscle stimulation with 5 minutes on and 5 minutes off, for up to one

hour, can enhance muscular mechanical properties (Kim, Roy et al. 2007). Although our study examined a very short duration stimulation of 10 minutes total, the insertion of a 5 minute recovery period showed significant attenuation of quadriceps fiber CSA. The change observed here was not statistically different than the change observed with a continuous stimulation, but the percent difference was slightly higher. Comparing the CSA data may not provide conclusive results regarding the role of a 5 minute recovery period, however, because the changes with rest-insertions were significantly different from hind limb suspension control, it indicates that recovery periods does influence muscular adaptation. It is possible the several short bouts of stimulation are required to enhance the response.

While muscular adaptation has been shown to be enhanced upon insertion of recovery periods during stimulation to mimic physiologic contractions and minimize fatigue, bone's adaptive response is more closely linked with concept of bone mechanosensitivity to fluid pressure gradients. It has been shown that mechanical loading increases fluid flow and diffusion inside bone (Knothe Tate, Steck et al. 2000). Many studies have demonstrated that osteocytes, while embedded in the rigid extracellular bone matrix, can respond to fluid flow. These responses have been shown to reach maximal effects within 5 minutes of flow stimulation, and subsequently level off (Klein-Nulend, Semeins et al. 1995). In our study, the evaluation of a recovery period during dynamic muscle stimulation did demonstrate a differential response in cortical bone morphology and mechanical strength properties. Cortical morphology showed higher significant recoveries with a 5 minute rest period, when compared with the continuous signal. Furthermore, mechanical testing revealed that the tissue stiffness and elastic modulus

were significantly different from disuse control, and that the rest-inserted signal induced a response that is significantly higher than the continuous response. Comparison of the maximal force/stress and failure force/stress also showed significant attenuation with the rest-inserted signal only, not the continuous signal. Together, these data show a stronger adaptive response in cortical bone with rest-insertion, rather than trabecular bone.

It has been unclear whether insertion of rest periods can strengthen both trabecular and cortical bone, as most studies have reported changes in cortical bone (Srinivasan, Weimer et al. 2002). Studies have suggested that mechanical loading regimes may induce cortical adaptation because of intracortical fluid pressure gradients, thus causing fluid to flow either towards the marrow or the periosteal surface (Qin, Kaplan et al. 2003). Due the highly viscous nature of intracortical fluid, it is believed that during repeated loading, osteocytes may experience inertial damping effects of the flow, and during high frequency loading, there may not be sufficient time to recover the inertial damping (Zhu, Lai et al. 1991). Thus, due to this concept of a saturation curve for bone mechanosensitivity, several studies have demonstrated the importance of inserting short-term and long-term recovery periods for enhancing the osteogenic response (Robling, Burr et al. 2001; Srinivasan, Weimer et al. 2002; LaMothe and Zernicke 2004). These studies examined the role of rest periods on the order of seconds to hours. In contrast, 10 seconds of rest inserted between 1 second bouts of high frequency, low magnitude whole body vibrations did not demonstrate improved skeletal response or increased mechanosensitivity (Xie, Jacobson et al. 2006). This may be explained by the lower strain magnitudes applied during stimulation. The results of our study showing the influence of a 5 minute rest period during a 10 minute stimulation are consistent with

many studies that show that cells are receptive first few minutes of loading, with relatively few load cycles per day (Rubin and Lanyon 1984). However, for further optimization of the osteogenic response, it may be important to investigate how rest insertions on the order of 10 seconds introduced between individual loading cycles of dynamic muscle contractions, because these regimes have been shown to enhance new bone formation (Srinivasan, Weimer et al. 2002). Further, it may be worthwhile to examine the musculoskeletal response to shorter, more frequent bouts of loading, since their osteogenic potential has been demonstrated, suggesting that recovery periods may restore mechanosensitivity (Robling, Hinant et al. 2002).

CHAPTER 5: CONCLUSIONS

SUMMARY

The two studies presented in this thesis investigated the role of dynamic muscle contractions as a preventive treatment for musculoskeletal disuse. Two different signal parameters were investigated for signal optimization to simultaneously target muscle atrophy and bone loss. The first study examined the frequency specificity of muscle stimulations on bone and muscle adaptation, and optimal responses were observed in the 20 Hz to 50 Hz range, as demonstrated by significant attenuation in trabecular and cortical bone morphology, bone mechanical strength, and muscle fiber cross sectional area. The second study examined the role of a inserting a 5-minute recovery period between two 5-minute bouts of a 20 Hz muscle stimulation. Trabecular bone morphology showed stronger attenuation with a continuous signal, however, cortical morphology showed stronger attenuation with the rest-inserted signal. Mechanical strength data and muscle morphology data showed that attenuation with the rest-inserted signal was significantly higher than the continuous signal. Thus, these data support the hypothesis that high frequency dynamic muscle contractions with rest-insertions have potential as a preventive treatment for disuse induced bone loss and muscle atrophy.

LIMITATIONS AND FUTURE DIRECTIONS

This study was initially designed with the stimulation of one hind limb so that contralateral comparisons could be made to evaluate the efficacy of this musculoskeletal treatment. However, the preliminary study demonstrated that application of electrical stimulation to one hind limb muscle significantly affected the response in bone and muscle of the contralateral limb. It is unclear why such systemic effects were observed,

however, it may be possible that stimulation of one limb activated of nerve depolarization of adjacent fiber and nerves, causing muscle twitching and ultimately resulting in an adaptive response that cannot be considered negligible when compared to disuse control animals. It is also possible that molecular event are triggered upon stimulation of one limb, and these event may subsequently affect other organ systems. Besides the potential systemic effects of the nerve response, other factors may have influenced the results during the experiment. For example, it is not clear whether the musculoskeletal adaptation was observed in response to the direct stimulation of muscle or due to the electric field. Future studies may isolate the electric field to one side of the animal during stimulation in order to rule out such possibilities. It may be relevant to include a sham control group for future experiments in which electrodes are place on the target muscle without stimulation of current flow. Other sources of systemic influences may include a biochemical or hormonal effect upon muscle activation. Verification of other systemic effects would require future studies to evaluate the changes in other tissues, such forelimb muscle and bone, and changes in serum proteins.

Muscle wet weight data showed variations which may be explained by error and inconsistency during weighing of muscles during the experiment. The order of magnitude of individual hind limb muscles is quite low and thus slight inconsistencies during dissections may be reflected as large variations. The time between tissue removal from the animal and actual weighing may also be important because the muscle begin to dry soon after dissection. The extent of drying may alter the weight values obtained. For reliable future studies it may be important to perform repeatability tests of muscle wet weights.

Muscle fiber CSA analysis revealed variations that may be explained by the lack of differentiating fiber types in this study. Slow twitch fibers are generally of smaller diameter as compared to fast twitch muscles which are much larger and are capable of generating greater levels of tension. Thus it will be important to evaluate the response of each fiber type to the dynamic muscle intervention, since different muscle types may display different dose-responses curves. Data to differentiate the response between muscle groups and fiber types may further elucidate the parameters optimal to particular types of tissue.

The mechanical testing performed in each of these studies demonstrated differences between stimulation groups, however, the stress strain curves displayed several regions, thus making it difficult to obtain conclusive results regarding the accuracy of the stiffness and elastic modulus of the bone tissue. This may have occurred due to rigid body movement during testing or possibly due to microcracking. In the case that microcracking occurred at several time points, it would not provide accurate data for determining the yield stress/force. Since the cause of the observation of multiple linear regions is unclear, the yield value could not be accurately reported.

The data presented in this study suggest the adaptive potential of muscle dynamics in musculoskeletal treatment. The underlying mechanism of bone adaptation via muscle contractions is proposed to be related to modulation in intramedullary pressure. Thus, to confirm this hypothesis it is important to investigate the changes in ImP this mouse model upon stimulation. In addition to quantification of ImP modulation, it will also be important to determine other factors that may regulate the musculoskeletal adaptation upon electrical stimulation of disused muscles. Since potential regulatory factors such as

ImP, matrix strain, tissue and cellular level deformations, and applied force due to muscle contractions are not isolated from each other in these experiments, a single mechanism of response cannot be determined. Therefore it will be important to perform measurements of bone strain, muscle force generation, and ImP modulation upon muscle stimulation in future studies. Data to confirm these results across various species may provide evidence for designing optimal treatments for human recovery. Further, the mouse model can be extended to evaluate molecular and genetic mechanism underlying this biomechanical intervention.

Akhter, M. P., D. M. Cullen, et al. (2001). "Bone biomechanical properties in prostaglandin EP1 and EP2 knockout mice." Bone **29**(2): 121-5.

Allen, D. L., R. R. Roy, et al. (1999). "Myonuclear domains in muscle adaptation and disease." Muscle Nerve **22**(10): 1350-60.

Baldi, J. C., R. D. Jackson, et al. (1998). "Muscle atrophy is prevented in patients with acute spinal cord injury using functional electrical stimulation." Spinal Cord **36**(7): 463-9.

Bassett, C. A. (1965). "Electrical effects in bone." Sci Am **213**(4): 18-25.

Belanger, M., R. B. Stein, et al. (2000). "Electrical stimulation: can it increase muscle strength and reverse osteopenia in spinal cord injured individuals?" Arch Phys Med Rehabil **81**(8): 1090-8.

Bensamoun, S. F., J. R. Hawse, et al. (2006). "TGFbeta inducible early gene-1 knockout mice display defects in bone strength and microarchitecture." Bone **39**(6): 1244-51.

Bergula, A. P., W. Huang, et al. (1999). "Femoral vein ligation increases bone mass in the hindlimb suspended rat." Bone **24**(3): 171-7.

Biering-Sorensen, F., H. H. Bohr, et al. (1990). "Longitudinal study of bone mineral content in the lumbar spine, the forearm and the lower extremities after spinal cord injury." Eur J Clin Invest **20**(3): 330-5.

Bloomfield, S. A. (1997). "Changes in musculoskeletal structure and function with prolonged bed rest." Med Sci Sports Exerc **29**(2): 197-206.

Buckwalter, J. A., M. J. Glimcher, et al. (1996). "Bone biology. I: Structure, blood supply, cells, matrix, and mineralization." Instr Course Lect **45**: 371-86.

Burger, E. H. and J. Klein-Nulend (1999). "Mechanotransduction in bone--role of the lacuno-canalicular network." Faseb J **13 Suppl**: S101-12.

Cameron, M. H. (2003). Physical Agents in Rehabilitation: From Research To Practice, Saunders.

Castro, M. J., D. F. Apple, Jr., et al. (1999). "Influence of complete spinal cord injury on skeletal muscle cross-sectional area within the first 6 months of injury." Eur J Appl Physiol Occup Physiol **80**(4): 373-8.

Cooper, R. R., J. W. Milgram, et al. (1966). "Morphology of the osteon. An electron microscopic study." J Bone Joint Surg Am **48**(7): 1239-71.

Cowin, S. C., S. Weinbaum, et al. (1995). "A case for bone canaliculi as the anatomical site of strain generated potentials." J Biomech **28**(11): 1281-97.

Delitto, A. and L. Snyder-Mackler (1990). "Two theories of muscle strength augmentation using percutaneous electrical stimulation." Phys Ther **70**(3): 158-64.

Dudley, G. A., M. R. Duvoisin, et al. (1989). "Alterations of the in vivo torque-velocity relationship of human skeletal muscle following 30 days exposure to simulated microgravity." Aviat Space Environ Med **60**(7): 659-63.

Dupont Salter, A. C., F. J. Richmond, et al. (2003). "Prevention of muscle disuse atrophy by low-frequency electrical stimulation in rats." IEEE Trans Neural Syst Rehabil Eng **11**(3): 218-26.

Ebashi, S. (1976). "Excitation-contraction coupling." Annu Rev Physiol **38**: 293-313.

Eser, P., A. Frotzler, et al. (2004). "Relationship between the duration of paralysis and bone structure: a pQCT study of spinal cord injured individuals." Bone **34**(5): 869-80.

Frey-Rindova, P., E. D. de Bruin, et al. (2000). "Bone mineral density in upper and lower extremities during 12 months after spinal cord injury measured by peripheral quantitative computed tomography." Spinal Cord **38**(1): 26-32.

Frost, H. M. (1963a). Bone Remodelling Dynamics. Springfield, IL.

Frost, H. M. (1982). "Mechanical determinants of bone modeling." Metab Bone Dis Relat Res **4**(4): 217-29.

Frost, H. M. (1990). "Skeletal structural adaptations to mechanical usage (SATMU): 2. Redefining Wolff's law: the remodeling problem." Anat Rec **226**(4): 414-22.

Gamble, J. G. (1988). The Musculoskeletal System: Physiological Basics. New York, Raven Press.

Giangregorio, L. and N. McCartney (2006). "Bone loss and muscle atrophy in spinal cord injury: epidemiology, fracture prediction, and rehabilitation strategies." J Spinal Cord Med **29**(5): 489-500.

Glucksmann, A. (1938). "Studies on boen mechanics in vitro. I. Influence of pressure on orientation of structure." The Anatomical Record **72**(Ch 2; Ch 4; Ch 6): 97-113.

Goldspink, G. (1964). "Increase in Length of Skeletal Muscle During Normal Growth." Nature **204**: 1095-6.

Gonyea, W., G. C. Ericson, et al. (1977). "Skeletal muscle fiber splitting induced by weight-lifting exercise in cats." Acta Physiol Scand **99**(1): 105-9.

Graupe, D. (2002). "An overview of the state of the art of noninvasive FES for independent ambulation by thoracic level paraplegics." Neurol Res **24**(5): 431-42.

Hanson, A. M., V. L. Ferguson, et al. (2005). "Comparison of tail-suspension and sciatic nerve crush on the musculoskeletal system in young-adult mice." Biomed Sci Instrum **41**: 92-6.

Hert, J., M. Liskova, et al. (1969). "Influence of the long-term, continuous bending on the bone. An experimental study on the tibia of the rabbit." Folia Morphol (Praha) **17**(4): 389-99.

Hsieh, Y. F. and C. H. Turner (2001). "Effects of loading frequency on mechanically induced bone formation." J Bone Miner Res **16**(5): 918-24.

Jacobs, C. R., C. E. Yellowley, et al. (1998). "Differential effect of steady versus oscillating flow on bone cells." J Biomech **31**(11): 969-76.

Jamsa, T., P. Jalovaara, et al. (1998). "Comparison of three-point bending test and peripheral quantitative computed tomography analysis in the evaluation of the strength of mouse femur and tibia." Bone **23**(2): 155-61.

Jee, W. S., T. J. Wronski, et al. (1983). "Effects of spaceflight on trabecular bone in rats." Am J Physiol **244**(3): R310-4.

Judex, S., L. R. Donahue, et al. (2002). "Genetic predisposition to low bone mass is paralleled by an enhanced sensitivity to signals anabolic to the skeleton." Faseb J **16**(10): 1280-2.

Judex, S., R. Garman, et al. (2004). "Genetically linked site-specificity of disuse osteoporosis." J Bone Miner Res **19**(4): 607-13.

Judex, S. and R. F. Zernicke (2000). "High-impact exercise and growing bone: relation between high strain rates and enhanced bone formation." J Appl Physiol **88**(6): 2183-91.
Kasser, J. R. (1996). General Knowledge. Illinois, American Academy of Orthopaedic Surgeons.
Kelly, P. J. and J. T. Bronk (1990). "Venous pressure and bone formation." Microvasc Res **39**(3): 364-75.
Kim, S. J., R. R. Roy, et al. (2007). "Electromechanical stimulation ameliorates inactivity-induced adaptations in the medial gastrocnemius of adult rats." J Appl Physiol **103**(1): 195-205.
Klein-Nulend, J., C. M. Semeins, et al. (1995). "Pulsating fluid flow increases nitric oxide (NO) synthesis by osteocytes but not periosteal fibroblasts--correlation with prostaglandin upregulation." Biochem Biophys Res Commun **217**(2): 640-8.
Knothe Tate, M. L., R. Steck, et al. (2000). "In vivo demonstration of load-induced fluid flow in the rat tibia and its potential implications for processes associated with functional adaptation." J Exp Biol **203**(Pt 18): 2737-45.
Koch, J. C. (1917). "The Laws of Bone Architecture." The American Journal of Anatomy **21**(Ch 6): 17-293.
LaMothe, J. M. and R. F. Zernicke (2004). "Rest insertion combined with high-frequency loading enhances osteogenesis." J Appl Physiol **96**(5): 1788-93.
Lanyon, L. E. (1973). "Analysis of surface bone strain in the calcaneus of sheep during normal locomotion. Strain analysis of the calcaneus." J Biomech **6**(1): 41-9.
Lanyon, L. E. (1974). "Experimental support for the trajectorial theory of bone structure." J Bone Joint Surg Br **56**(1): 160-6.
Lanyon, L. E., W. G. Hampson, et al. (1975). "Bone deformation recorded in vivo from strain gauges attached to the human tibial shaft." Acta Orthop Scand **46**(2): 256-68.
Lanyon, L. E. and R. N. Smith (1969). "Measurements of bone strain in the walking animal." Res Vet Sci **10**(1): 93-4.
LeBlanc, A., C. Marsh, et al. (1985). "Bone and muscle atrophy with suspension of the rat." J Appl Physiol **58**(5): 1669-75.
Lieber, R. L. (1986). "Skeletal muscle adaptability. I: Review of basic properties." Dev Med Child Neurol **28**(3): 390-7.
Lieber, R. L. (1986). "Skeletal muscle adaptability. III: Muscle properties following chronic electrical stimulation." Dev Med Child Neurol **28**(5): 662-70.
Lieber, R. L. (1988). "Comparison between animal and human studies of skeletal muscle adaptation to chronic stimulation." Clin Orthop Relat Res(233): 19-24.
Lieber, R. L., T. D. Ferro, et al. (1988). "Differential effects of 10-Hz and 50 Hz-stimulation of the tibialis anterior on the ipsilateral, unstimulated soleus muscle." Exp Neurol **100**(2): 426-35.
Liskova, M. and J. Hert (1971). "Reaction of bone to mechanical stimuli. 2. Periosteal and endosteal reaction of tibial diaphysis in rabbit to intermittent loading." Folia Morphol (Praha) **19**(3): 301-17.
Loughna, P., G. Goldspink, et al. (1986). "Effect of inactivity and passive stretch on protein turnover in phasic and postural rat muscles." J Appl Physiol **61**(1): 173-9.

Loughna, P. T., S. Izumo, et al. (1990). "Disuse and passive stretch cause rapid alterations in expression of developmental and adult contractile protein genes in skeletal muscle." Development **109**(1): 217-23.

Martin, R. B. and D. B. Burr (1989). Structure, Function, and Adaptation of Compact Bone. New York, Raven Press.

Martin, R. B., D. B. Burr, et al. (1998). Skeletal Tissue Mechanics, Springer-Verlag New York, Inc.

Mattiello-Sverzut, A. C., L. C. Carvalho, et al. (2006). "Morphological effects of electrical stimulation and intermittent muscle stretch after immobilization in soleus muscle." Histol Histopathol **21**(9): 957-64.

Midura, R. J., C. J. Dillman, et al. (2005). "Low amplitude, high frequency strains imposed by electrically stimulated skeletal muscle retards the development of osteopenia in the tibiae of hindlimb suspended rats." Med Eng Phys **27**(4): 285-93.

Modlesky, C. M., J. M. Slade, et al. (2005). "Deteriorated geometric structure and strength of the midfemur in men with complete spinal cord injury." Bone **36**(2): 331-9.

Morey-Holton, E. R. and R. K. Globus (2002). "Hindlimb unloading rodent model: technical aspects." J Appl Physiol **92**(4): 1367-77.

Mosley, J. R. and L. E. Lanyon (1998). "Strain rate as a controlling influence on adaptive modeling in response to dynamic loading of the ulna in growing male rats." Bone **23**(4): 313-8.

Nordin, M. and V. H. Frankel (2001). Basic Biomechanics of the Musculoskeletal System, Lippincott Williams & Wilkins.

Nordsletten, L., T. S. Kaastad, et al. (1994). "Muscle contraction increases the in vivo structural strength to the same degree in osteopenic and normal rat tibiae." J Bone Miner Res **9**(5): 679-85.

O'Connor, J. A., L. E. Lanyon, et al. (1982). "The influence of strain rate on adaptive bone remodelling." J Biomech **15**(10): 767-81.

Pavy-Le Traon, A., M. Heer, et al. (2007). "From space to Earth: advances in human physiology from 20 years of bed rest studies (1986-2006)." Eur J Appl Physiol **101**(2): 143-94.

Piekarski, K. and M. Munro (1977). "Transport mechanism operating between blood supply and osteocytes in long bones." Nature **269**(5623): 80-2.

Prentice, W. E. (2002). Therapeutic Modalities for Physical Therapists, McGraw Hill.

Qin, L., H. J. Appell, et al. (1997). "Electrical stimulation prevents immobilization atrophy in skeletal muscle of rabbits." Arch Phys Med Rehabil **78**(5): 512-7.

Qin, Y. X., T. Kaplan, et al. (2003). "Fluid pressure gradients, arising from oscillations in intramedullary pressure, is correlated with the formation of bone and inhibition of intracortical porosity." J Biomech **36**(10): 1427-37.

Qin, Y. X., W. Lin, et al. (2002). "The pathway of bone fluid flow as defined by in vivo intramedullary pressure and streaming potential measurements." Ann Biomed Eng **30**(5): 693-702.

Qin, Y. X., C. T. Rubin, et al. (1998). "Nonlinear dependence of loading intensity and cycle number in the maintenance of bone mass and morphology." J Orthop Res **16**(4): 482-9.

Reich, K. M., C. V. Gay, et al. (1990). "Fluid shear stress as a mediator of osteoblast cyclic adenosine monophosphate production." J Cell Physiol **143**(1): 100-4.
Robling, A. G., D. B. Burr, et al. (2001). "Recovery periods restore mechanosensitivity to dynamically loaded bone." J Exp Biol **204**(Pt 19): 3389-99.
Robling, A. G., K. M. Duijvelaar, et al. (2001). "Modulation of appositional and longitudinal bone growth in the rat ulna by applied static and dynamic force." Bone **29**(2): 105-13.
Robling, A. G., F. M. Hinant, et al. (2002). "Shorter, more frequent mechanical loading sessions enhance bone mass." Med Sci Sports Exerc **34**(2): 196-202.
Rubin, C., A. S. Turner, et al. (2002). "Quantity and quality of trabecular bone in the femur are enhanced by a strongly anabolic, noninvasive mechanical intervention." J Bone Miner Res **17**(2): 349-57.
Rubin, C., G. Xu, et al. (2001). "The anabolic activity of bone tissue, suppressed by disuse, is normalized by brief exposure to extremely low-magnitude mechanical stimuli." Faseb J **15**(12): 2225-9.
Rubin, C. T. and L. E. Lanyon (1984). "Regulation of bone formation by applied dynamic loads." J Bone Joint Surg Am **66**(3): 397-402.
Rubin, C. T. and L. E. Lanyon (1985). "Regulation of bone mass by mechanical strain magnitude." Calcif Tissue Int **37**(4): 411-7.
Salmons, S. and J. Henriksson (1981). "The adaptive response of skeletal muscle to increased use." Muscle Nerve **4**(2): 94-105.
Shackelford, L. C., A. D. LeBlanc, et al. (2004). "Resistance exercise as a countermeasure to disuse-induced bone loss." J Appl Physiol **97**(1): 119-29.
Simske, S. J., A. R. Greenberg, et al. (1991). "Effects of suspension-induced osteopenia on the mechanical behaviour of mouse long bones." J Mater Sci Mater Med **2**(1): 43-50.
Sinacore, D. R., A. Delitto, et al. (1990). "Type II fiber activation with electrical stimulation: a preliminary report." Phys Ther **70**(7): 416-22.
Skold, C., L. Lonn, et al. (2002). "Effects of functional electrical stimulation training for six months on body composition and spasticity in motor complete tetraplegic spinal cord-injured individuals." J Rehabil Med **34**(1): 25-32.
Squire, J. (1981). The Structural Basis of Muscular Contraction. New York, Plenum Press.
Squire, M., A. Brazin, et al. (2007). "Baseline bone morphometry and cellular activity modulate the degree of bone loss in the appendicular skeleton during disuse." Bone.
Srinivasan, S., D. A. Weimer, et al. (2002). "Low-magnitude mechanical loading becomes osteogenic when rest is inserted between each load cycle." J Bone Miner Res **17**(9): 1613-20.
Tesch, P. A., H. E. Berg, et al. (1991). "Muscle strength and endurance following lowerlimb suspension in man." Physiologist **34**(1 Suppl): S104-6.
Thompson, D. W. (1917). On Growth and Form. London, Cambridge University Press.
Turner, C. H. and D. B. Burr (1993). "Basic biomechanical measurements of bone: a tutorial." Bone **14**(4): 595-608.
Turner, C. H., M. R. Forwood, et al. (1994). "Mechanotransduction in bone: do bone cells act as sensors of fluid flow?" Faseb J **8**(11): 875-8.

Vico, L., D. Chappard, et al. (1987). "Effects of a 120 day period of bed-rest on bone mass and bone cell activities in man: attempts at countermeasure." Bone Miner **2**(5): 383-94.

Wallace, J. M., R. M. Rajachar, et al. (2007). "Exercise-induced changes in the cortical bone of growing mice are bone- and gender-specific." Bone **40**(4): 1120-7.

Warden, S. J. and C. H. Turner (2004). "Mechanotransduction in the cortical bone is most efficient at loading frequencies of 5-10 Hz." Bone **34**(2): 261-70.

Wei, C. N., Ohira, et al. (1998). "Does electrical stimulation of the sciatic nerve prevent suspension-induced changes in rat hindlimb bones?" Jpn J Physiol **48**(1): 33-7.

Weinbaum, S., S. C. Cowin, et al. (1994). "A model for the excitation of osteocytes by mechanical loading-induced bone fluid shear stresses." J Biomech **27**(3): 339-60.

Widmaier, E. P., H. Raff, et al. (2004). Human Physiology: The Mechanism of Body Function, McGraw-Hill.

Wilmet, E., A. A. Ismail, et al. (1995). "Longitudinal study of the bone mineral content and of soft tissue composition after spinal cord section." Paraplegia **33**(11): 674-7.

Winet, H. (2003). "A bone fluid flow hypothesis for muscle pump-driven capillary filtration: II. Proposed role for exercise in erodible scaffold implant incorporation." Eur Cell Mater **6**: 1-10; discussion 10-1.

Wolff, J. (1892). The Law of Bone Remodeling. (Translation of Wolff's Das Gesetz der Transformation der Knochen by P. Maquet and R. Furlong). Berlin, Spring-Verlag.

Wronski, T. J. and E. R. Morey (1983). "Effect of spaceflight on periosteal bone formation in rats." Am J Physiol **244**(3): R305-9.

Xie, L., J. M. Jacobson, et al. (2006). "Low-level mechanical vibrations can influence bone resorption and bone formation in the growing skeleton." Bone **39**(5): 1059-66.

Zehnder, Y., M. Luthi, et al. (2004). "Long-term changes in bone metabolism, bone mineral density, quantitative ultrasound parameters, and fracture incidence after spinal cord injury: a cross-sectional observational study in 100 paraplegic men." Osteoporos Int **15**(3): 180-9.

Zerath, E., F. Canon, et al. (1995). "Electrical stimulation of leg muscles increases tibial trabecular bone formation in unloaded rats." J Appl Physiol **79**(6): 1889-94.

Zhang, P., M. Su, et al. (2006). "Knee loading dynamically alters intramedullary pressure in mouse femora." Bone.

Zhu, W., W. M. Lai, et al. (1991). "The density and strength of proteoglycan-proteoglycan interaction sites in concentrated solutions." J Biomech **24**(11): 1007-18.